Contract No:

This document was prepared in conjunction with work accomplished under Contract No. DE-AC09-08SR22470 with the U.S. Department of Energy (DOE) Office of Environmental Management (EM).

We put science to work.™

Savannah River
National Laboratory ™
OPERATED BY SAVANNAH RIVER NUCLEAR SOLUTIONS

A U.S. DEPARTMENT OF ENERGY NATIONAL LABORATORY • SAVANNAH RIVER SITE • AIKEN, SC

Characterization of Laboratory Prepared Concrete Pastes Exposed to High Alkaline and High Sodium Salt Solutions

C. A. Langton

June, 2016

SRNL-STI-2016-00214, Revision 0

CBP-RP-2015-013, Revision 0

SRNL.DOE.GOV

DISCLAIMER

Printed in the United States of America

Prepared for
U.S. Department of Energy

Keywords: Concrete Durability
Alkali Silica Reaction
Saltstone Disposal Unit
SDU Concrete

Retention: *Permanent*

Characterization of Laboratory Prepared Concrete Pastes Exposed to High Alkaline and High Sodium Salt Solutions

C. A. Langton

June, 2016

Prepared in conjunction with work accomplished under contract number DE-AC09-08SR22470 with the U.S. Department of Energy (DOE) Office of Environmental Management (EM).

Savannah River National Laboratory™

OPERATED BY SAVANNAH RIVER NUCLEAR SOLUTIONS

REVIEWS AND APPROVALS

AUTHORS:

C. A. Langton, Engineering and Chemical Process Technology Research Programs Date

TECHNICAL REVIEW:

E. Samson, SIMCO Technologies, Inc. Date

W.P. Kubilius, Engineering and Chemical Process Technology Research Programs Date

APPROVALS:

H. H. Burns, Cementitious Barriers Project Manager, SRNL, Date

E. N. Hoffman, Manager, SRNL, Engineering Process Development Date

D. Dooley, Director, Engineering and Chemical Process Technology Research Programs Date

ACKNOWLEDGEMENTS

SIMCO Technology Inc. personnel provided samples characterized in this study. D. M. Missimer, SRNL, provided x-ray diffraction patterns for subsamples collected from the as received samples. H. M. Ajo, SRNL, performed SEM characterization as did Dr. L. SARAF, Advanced Microscopy Laboratory, Clemson University. S. P. Simner and N. F. Chapman, Savannah River Remediation, E. Samson, SIMCO Technologies, Inc., and W. P. Kubilius and D. L. McClane, SRNL provided technical reviews for this document. DOE-EM 21 provided funding for this study through the Cementitious Barriers Partnership Project.

EXECUTIVE SUMMARY

The objective of this study was to identify potential chemical degradation mechanisms for the Saltstone Disposal Unit (SDU) concretes, which over the performance life of the structures may be exposed to highly alkaline sodium salt solutions containing sulfate, hydroxide, and other potentially corrosive chemicals in salt solution and saltstone flush water, drain water, leachate and / or pore solution. The samples analyzed in this study were cement pastes prepared in the SIMCO Technologies, Inc. concrete laboratory. They were based on the paste fractions of the concretes used to construct the Saltstone Disposal Units (SDUs). SDU 1 and 4 concrete pastes were represented by the PV1 test specimens. The paste in the SDU 2, 3, 5, and 6 concrete was represented by the PV2 test specimens. SIMCO Technologies, Inc. selected the chemicals and proportions in the aggressive solutions to approximate proportions in the saltstone pore solution [2, 3, 5, and 6].

These test specimens were cured for 56 days in curing chamber before being immersed in aggressive solutions. After exposure, the samples were frozen to prevent additional chemical transport and reaction. Selected archived (retrieved from the freezer) samples were sent to the Savannah River National Laboratory (SRNL) for additional characterization using x-ray diffraction (XRD), scanning electron microscopy (SEM), and energy dispersive x-ray (EDX) spectroscopy. Characterization results are summarized in this report. In addition, a correlation between the oxide composition of the pastes and their chemical durability in the alkaline salt solutions is provided.

It is important to understand that the materials utilized in the exposure testing are not completely representative of the SDU6 concrete in that: (1) they contain no sand or aggregate, (2) the lack of aggregate can impact the de-agglomeration and dispersion of components, such as silica fume, during mixing, and (3) pre-exposure curing time (56 days at 100 % relative humidity) was significantly less than would be anticipated in the field. Additionally, SDU concrete in the field will be predominantly in contact with cured saltstone rather than immersed in saltstone pore solutions, and the SDU concrete will be lined or coated with a chemically resistant barrier between the it and saltstone.

The SIMCO Technologies, Inc. test protocol can be considered an accelerated method for comparing various paste compositions with respect to susceptibility for chemical degradation of concretes made with these pastes. Immersion testing of the concrete paste samples in simulant pore solution provides an essentially infinite supply of aggressive chemical species and water for formation of hydrated reactions products and through which the chemicals are transported into the paste samples. Also it should be noted that the paste fraction makes up about 20 volume percent of the actual concrete so the expression of damage for paste samples is not expected to be the same as that for concrete which contains about 80 volume percent non porous quartz sand and granite aggregate. A complete description of the SIMCO test program which was funded by the Cementitious Barriers Partnership is provided elsewhere [2, 4, and 5].

The results from exposure of the paste specimens to two of five solutions evaluated in the SIMCO Technologies Inc. study are discussed in this report. A complete description of the SIMCO Technologies Inc., test program funded by the Cementitious Barriers Partnership is provided elsewhere [2, 4, and 5].

Alteration / degradation of PV1 paste samples immersed in Solutions 2 (0.15 M Na_2SO_4 and 0.5M NaOH) and 4 (0.15 M Na_2SO_4, 0.5M NaOH and 3.0 M $NaNO_3$) for one year was limited to a depth of less than about 100 µm. This was also the case for samples made with 100 % Portland Type I/II cement (PV1b) and 100 % Portland cement type V (PV2b). The interior regions of these samples appeared to be unaffected after immersion in these solutions for one year. The PV1 paste is a 60/40 blend of Portland Type I/II cement and slag cement formerly referred to as ground granulated blast furnace slag. This paste represents the paste fraction of the paste used in the SDU 1 and 4 concrete.

On the other hand, the PV2 paste samples immersed in Solutions 2 and 4 for one year were severely degraded, i.e, cracked. The sample immersed in Solution 4 was more degraded than the one exposed to Solution 2. Based on scanning electron microcopy of immersed PV2 samples, the cracking appears to be caused by alkali silica reactivity of silica fume agglomerates in the PV2 paste. Alkali silica reactivity of agglomerated silica fume has been reported in the literature as a cause of concrete degradation. The PV 2 paste is a 30:41:23:7 quaternary blend of Portland Type V cement:slag cement:Class F fly ash: silica fume. This paste represents the paste in the concrete used to construct SDU 2, 3, 5, and 6. Additional testing is required to determine whether laboratory and/or field produced concrete used to construct SDU 2, 3, 5, and 6 contains silica fume agglomerates and is susceptible to ASR.

Ettringite, a low density phase associated with expansion and cracking characteristic of sulfate attack, was observed in samples that were affected by ASR but did not appear to be the cause cracking. Although sodium nitrate is not usually associated with chemical alteration of cement paste or concrete, dendritic evaporate sodium nitrate crystals were observed on planes of weakness perpendicular to the axis of the PV 2 paste disks immersed in the Solution 4 which contained 3 M sodium nitrate. These crystals may have formed during sample storage and accentuated the cracking due to expansion.

The bulk oxide composition of the pastes was identified as a parameter that can be correlated to potential for chemical degradation / durability in the chemical environments evaluated. Paste samples (PV1, 1b, and 2b) with high CaO / SiO_2 ratios, e.g., 1.9 to 3.1 were more durable in highly alkaline aggressive solutions than the paste sample, PV2, which contained silica fume agglomerates and had a ratio of 0.8.

ASR typically involves reaction between the hydroxyl ions in the alkaline pore solution in the concrete and reactive forms of silica in the aggregate (eg: chert, quartzite, opal, strained quartz crystals, etc.). Under common exposure conditions, alkali-silica reaction can be controlled for concrete exposed to typical environmental conditions by incorporating certain supplementary cementitious materials, e.g., silica fume, fly ash, and ground granulated blast-furnace slag, which in proper proportions can significantly reduce or eliminate expansion due to alkali-silica reactivity. In addition, lithium salts have been used to reduce ASR in concrete. These remedies should be evaluated for concrete exposed to the highly alkaline corrosive solutions encountered in the SDU application.

Because these samples appeared to be degraded by at least two mechanisms, i.e., cracking resulting from ASR expansive gel formation and external sulfate attack as indicated by gypsum formation throughout the matrix, the benefit of Type V, high sulfate resistant cement, in the PV2 paste requires further evaluation especially if silica fume is used in future SDU concrete mixes. The role of $NaNO_3$ in the degradation of PV2 is unclear.

The samples examined in this evaluation were cured in sealed containers for only 56 days prior to immersion in the aggressive alkaline salt solutions. If the samples had been cured for a longer time at 100 % relative humidity or in saturated lime water, they would be expected to be more mature and somewhat less susceptible to chemical degradation. The presence of portlandite in all of the exposed samples supports the idea that longer curing times under moist conditions would have resulted in additional hydration and pozzolanic reactions and hence may have improved resistance to chemical attack.

Conditions encountered in radioactive waste disposal scenarios can be significantly different than conditions for which engineering codes and standards are based. Durability of concrete and other cementitious materials must be evaluated for chemical environments expected in the disposal setting. If exposure conditions are outside those used to develop relevant codes and standards, the new test protocols are required.

TABLE OF CONTENTS

LIST OF TABLES

LIST OF FIGURES

LIST OF ACRONYMS AND ABBREVIATIONS

ASR	Alkali silica reaction
ASTM	American Society for Testing and Materials International
CBP	Cementitious Barriers Partnership
CV	Coefficient of variance
d	day
$D_{(OH)}$	Hydroxide diffusivity
DOE	US Department of Energy
EDX	Energy dispersive x-ray spectroscopy
GGBFS	Ground granulated blast furnace slag (synonymous with slag cement)
I2	Immersion Solution 2 (same as S2)
I4	Immersion Solution 4 (same as S4)
L	liter
M/L	Moles /liter
OPC	Ordinary Portland cement
PV1	Paste for concrete used to construct SDU1
PV2	Paste for concrete used to construct SDU2
S2	Immersion Solution 2 (same as I2)
S4	Immersion Solution 4 (same as I4)
SDU	Saltstone Disposal Unit
SEM	Scanning electron microscope
SRNL	Savannah River National Laboratory
SRS	Savannah River Site
w/b	Water to binder ratio by weight (binder = cement + pozzolan + slag)
w/c	Water to cement ratio by weight
XRD	X-ray diffraction

1.0 INTRODUCTION

1.1 Objective

The objective of this study was to characterize samples of cementitious paste prepared by SIMCO Technologies, Inc. as part of the Cementitious Barriers Partnership (CBP) Experimental Program Task12: Evaluation of the Chemical Durability of the Concrete Used to Construct the Savannah River Site (SRS) Saltstone Disposal Units (SDUs). The exposure testing was intended to improve understanding interactions between cementitious materials immersed in solutions containing one or more sodium salts, e.g., nitrite, nitrate, sulfate and carbonate at different pH conditions. Results were also intended to support SIMCO Inc. chemical degradation modeling.

This report provides mineralogy and microstructure characterization of four samples from the SIMCO Technology Inc. test program.

1.2 Background

Two pastes, PV1 and PV2 were prepared by SIMCO Technology Inc., personnel with compositions representing the binders (matrix) in the concrete mixes used to construct SDUs 1 and 2, respectively. The same concrete used for SDU 1 was used for SDU 4. The concrete used for SDU 2 was also used for SDUs 3, 5, and 6. The ingredients and proportions in the SDU 1 and SDU 2 concrete are provided in Table 1-1 [2]. SDU 1 and 4 are the same composition, and the concretes used for SDU 2, 3, 5, and 6 the same.

Selected physical properties of the two concretes are provided in Table 1-2 [2]. Oxide compositions of the cements and supplementary cementitious materials used to prepare test samples are provided in Tabled 1-3 [2]. The sample preparation, exposure testing, and results of exposure testing are provided in SIMCO Technologies, Inc. reports [2, 5].

Approximately 1.5 L batches of PV1 and PV2 paste were prepared according to ASTM C305 by SIMCO Technologies, Inc. Proportions of the ingredients in these pastes are provided in Table 1-4. The samples were cast in 100 mm (diameter) by 200 mm (height) (4 x 8 inch) cylinders and cured for 56 days in sealed containers. Additional details regarding the concrete compositions, sources of the various ingredients used for the SDU concretes, and physical and hydraulic properties of the concretes are provided elsewhere [1, 3, and 4].

Disks 100 mm x 25 mm (4 x 1 inch) were cut from the as cast samples and immersed in 5 different solutions. These immersion solutions were prepared by SIMCO Technologies, Inc., and the immersion testing was performed by SIMCO Technologies, Inc. Details of the sample preparation and immersion testing are provided elsewhere [2, 5].

The compositions of the solutions in which the paste samples were immersed are provided in Table 1-5. These solutions were prepared by SIMCO Technologies, Inc. The solution compositions were based on saltstone pore solution analyses. A series of immersion solutions were prepared for a systematic approach to evaluating the effect of the various components in the pore solution and is described elsewhere [2]. Figure 1-1 illustrates the configuration of the disks in the 25 L immersion tanks. Samples were exposed for 12 months. After exposure, SIMCO Technologies characterized the samples for physical and transport properties. Results are presented in CBP Task 12 – Experimental Study: OPC Paste Samples Exposed to Aggressive Solutions [2]. Archived samples were frozen to mitigate further migration of soluble salts and further alkali salt damage.

This report contains characterization results for four archived samples, PV1 and PV2 pastes immersed in Solutions 2 and 4. Table 1-6 provides a correlation between the SIMCO exposure sample labels and the sample identification used for SRNL characterization studies. A detailed description of the testing and results for the complete data set is presented elsewhere [2].

Table 1-1. Ingredients and proportions in concrete and paste specimens prepared by SIMCO Technologies, Inc. which represents the concrete and paste in SDU 1 and SDU 2 [1, 2].

Ingredient	Saltstone Disposal Units 1		Saltstone Disposal Unit 2	
	Concrete Proportions (kg/m^3)	PV1 Binder (wt. %)	Concrete Proportions (kg/m^3)	PV2 Binder (wt. %)
Type I/II cement	255	60	--	--
Type V cement	--	--	121	30
GGBFS	169	40	162	40
Fly Ash F	--	--	95	23
Silica Fume	--	--	27	7
Sand	692	--	548	--
Coarse aggregates No. 6/7 Stone	1,095	--	1,111	--
Water / Binder	0.38	0.40	0.38	0.40
Air	6 vol. %	6 vol. %	6 vol. %	6 vol. %
MicroAir (BASF) Polyheed N (BASF) Glenium 3030 (BASF	1.2 390 936	--	3.1 205 232	--
Total Binder kg/m^3 concrete	425	100	405	100

Table 1-2. Selected properties of SDU 1 and 2 concretes [1, 4]

Property	SDU 1 Concrete	SDU 2 Concrete
Compressive strength @ 28 d (MPa) Coefficient of Variance (%)	62.6 0.8	49.9 10.5
Density (kg/m^3)	2354	2302
Porosity @ 28 d	11.4	13.1
$D_{(OH)}$ @ 28 d (m^2/s)	5.18 E-11	3.28 E-11
@ 1 yr	3.7 E-11	2.00 E-11
@ 2 yr	3.21 E-11 (Standard Deviation = 0.19)	0.27 E-11 (Standard Deviation = 0.05)
Permeability @ 2 yr (m^2) Hydraulic Conductivity (cm/s)	0.68 E-22 (Standard Deviation = 0.032) 5E-12	0.65 (Standard Deviation = 0.064) 2 E-12

Table 1-3. Chemical composition of cement and pozzolan ingredients in PV1 and PV2 pastes [2].

Oxides	Type I/II cement	Type V cement	GGBFS	Force 10000 Silica Fume	Class F Fly Ash
	Lafarge	Lehigh	Holcim	Grace	SEFA
CaO	64.8	63.8	37.8	0.60	1.32
SiO_2	20.9	21.0	39.6	95.0	54.5
Al_2O_3	4.80	3.82	7.61	0.18	28.1
Fe_2O_3	3.43	4.75	0.47	0.07	8.65
SO_3	1.75	1.15	1.05	0.18	<0.1
MgO	1.05	2.60	12.2	0.22	1.19
K_2O	0.54	0.61	0.47	0.48	2.82
Na_2O	0.22	0.15	0.28	0.18	0.41
LOI	1.13	0.84	-0.45	3.32	1.41

Table 1-4. Ingredients and proportions in PV1, PV2 and two neat cement pastes prepared and evaluated by SIMCO Technologies, Inc. [2].

Binder Ingredient	PV1 Binder (wt. %)	PV1b Type I/II Reference Binder* (wt. %)	PV 2 Binder (wt. %)	PV2b Type V Reference Binder* (wt. %)
Type I/II cement	60	100	--	--
Type V cement	--	--	30	100
GGBFS	40	--	40	--
Fly Ash F	--	--	23	--
Silica Fume	--	--	7	--
Water / Total Cementitious Ingredients	0.38	0.40	0.38	0.40
Air	6	5	6	5

*These samples are discussed in this report but samples were not characterized at SRNL. Photos of these samples courtesy of SIMCO Technologies, Inc.

Table 1-5. Composition of immersion/exposure solutions and major components of pore solution from simulated saltstone waste forms.

	Immersion solution		**Pore Solution**			
Salts	**Solution 2 [2]**	**Solution 4 [2]**	**Simulated MCU Saltstone cured 28 days [6]**	**Saltstone* prepared by SIMCO cured 28 days [3]**	**Saltstone* prepared by SIMCO cured 123 days [3]**	**Saltstone prepared by SIMCO [5]**
	(mmol)					
Na_2SO_4	150	150	112	120	139	124
NaOH	500	500	384	485	151	130
$NaNO_3$	0	3000	3552**	3516**	3152**	3713**
Na_2CO_3	0	0	47	115	97	53

* ~ 5 M Na salt solution composition
** N (NO_3^- plus NO_2^-)

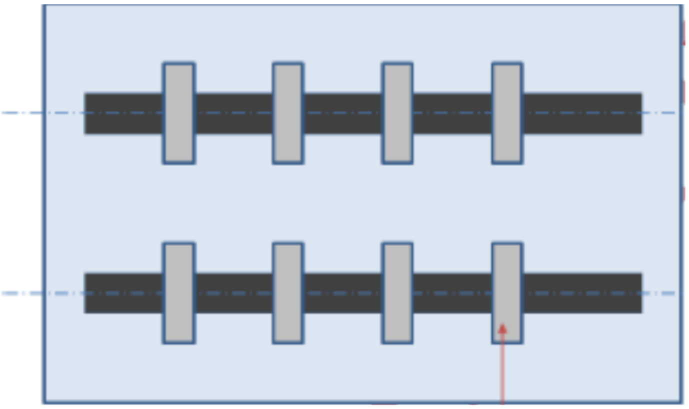

Plan View: 25 L Immersion Tank with multiple samples in racks

Figure 1-1. Schematic of immersion tank configuration showing racks holding paste sample disks. Top: plan view. Bottom: side view (courtesy of SIMCO Technologies, Inc.) [2, 5].

Table 1-6. Sample ID and correlation of pastes to SDUs.

SIMCO Sample ID*	**SRNL Sample ID**	**SDU Concrete Paste**	**Exposure Solution ID**
PV 1 Im2 @ 1 yr	PV1S2	1, 4	2
PV 1 Im4 @ 1 yr	PV1S4	1, 4	4
PV2 I2 (6) @ 1 yr.	PV2S2	2, 3, 5, 6	2
PV2 I4 (5) @ 1 yr.	PV2S4	2, 3, 5, 6	4

2.0 CHARACTERIZATION OF IMMERSED PV1 AND PV2 PASTES

2.1 Visual Examination

Photographs (courtesy of SIMCO Technologies, Inc.) of the PV1 and PV2 samples were taken by SIMCO Technologies, Inc., personnel immediately after they were removed from Solutions 2 and 4 and are provided in Figure 2-1 and 2-2, respectively [2, 5].

Photographs of control samples, i.e., neat Portland Type I/II cement pastes PV1b and neat Portland Type V cement pastes PV2b exposed to Solutions 2 and 4 were taken by SIMCO Technologies Inc. personnel immediately after removal from the immersion solutions and are also shown in Figure 2-1 and 2-2, respectively. These Portland cement-only pastes were included in the experimental program as reference materials to evaluate the effects of cement type (I/II versus V) on the resistance of the paste to sulfate attack. Based on the photographs taken from the SIMCO report, these paste were intact and were similar to the PV1 samples exposed to Solutions 2 and 4 [2, 5].

Samples sent to SRNL for more detailed characterization are shown in Figure 2-3. As received samples of PV1 and PV2 pastes that were cured for 56 days, prepared for immersion testing, and then immersed in solutions S2 and S4 for 1 year were photographed upon arrival from SIMCO Technologies Inc. Between the end of the exposure testing and retrieval of archived samples at SIMCO, these samples were stored in a freezer to stop chemical and mineralogical changes. Freezing and subsequent thawing and drying may have accentuated the visual expression of damage that occurred during immersion.

Prisms cut (by SIMCO personnel) from sample of the PV1 paste disks immersed in Solution 2 or 4 showed little degradation (Figure 2-3 top). However, the disk samples of PV 2 immersed in Solutions 2 and 4 were significantly degraded (Figure 2-3 middle and bottom, respectively). PV2 immersed in Solution 2 (0.15 M Na_2SO_4 and 0.5M NaOH) showed less damage than PV2 immersed in Solution 4 (0.15 M Na_2SO_4, 0.5 M NaOH, and 3.0 M $NaNO_3$). The three ingredients in Solution 4 approximate the concentrations of these chemicals in saltstone pore solution [2, 5, and 6]. Chemical analyses of simulated saltstone pore solutions are provided elsewhere [6].

(a) PV1
Type I/II cement + GGBFS,
w/b = 0.38

(b) PV1b
Type I/II Cement (neat)
w/c = 0.40

(c) PV2
Type V cement + GGBFS + Silica Fume + Class F fly ash, w/b = 0.38

(d) PV2b
Type V Cement (neat)
w/c = 0.40

Figure 2-1. Paste samples PV1, Type I/II paste, PV2, and Type V paste immersed in Solution 2 (0.15 M Na_2SO_4 and 0.5M NaOH) for 1 year. (Images are courtesy of SIMCO Technologies, Inc.)

(a) PV1
Type I/II cement + GGBFS
w/b = 0.38

(b) PV1b
Type I/II Cement (neat)
w/c = 0.40

(c) PV2
Type V cement + GGBFS + Silica Fume + Class F fly ash, w/b = 0.38

(d) PV2b
Type V Cement (neat)
w/c = 0.40

Figure 2-2. Paste samples immersed in Solution 4 (0.15 M Na_2SO_4, 0.5 M NaOH, and 3.0 M $NaNO_3$) for 1 year. (Images are courtesy of SIMCO Technologies, Inc.)

	
Prisms cut from PV1 Im2 disk (SDU 1 & 4) after immersion in Solution 2 (Na sulfate and hydroxide) for 1 yr.	Prisms cut from PV1 Im4 disk (SDU 1 & 4) after immersion in Solution 4 (Na sulfate, hydroxide and nitrate) for 1 yr.
	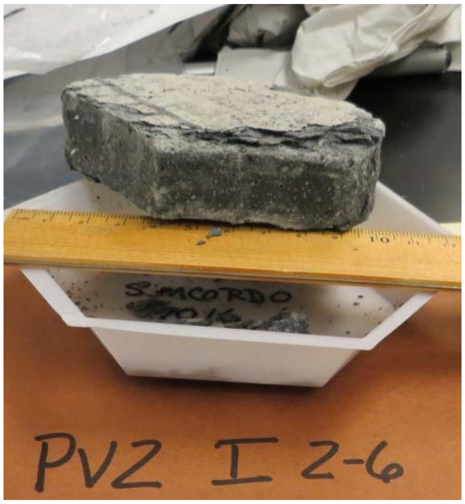
PV2 I2 disk, replicate 6 after immersion in Solution 2 (Na sulfate and hydroxide) for 1 yr.	
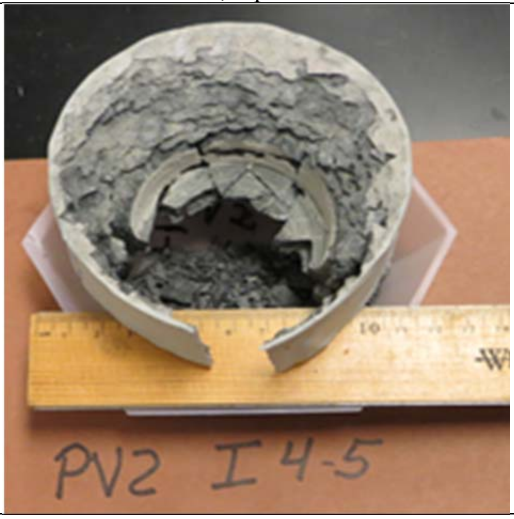	
PV2 I4 disk replicate 5 after immersion in Solution 4 (Na sulfate, hydroxide and nitrate) for 1 yr.	

Figure 2-3. **Paste samples, PV1 and PV2 after 1 year immersion in simplified simulated saltstone pore solution as received from SIMCO Technologies, Inc. Samples in the bottom row were frozen after removal from the immersion solutions to prevent additional chemical changes.**

2.2 Microstructure and Particle Morphology

These four paste samples were characterized by x-ray diffraction (XRD) and scanning electron microscopy / energy dispersive x-ray spectroscopy (SEM/EDX).

Paste 1 Solution 2. The PV1 is a binary blend consisting of Portland cement Type I/II and slag cement. Degradation of the PV1 specimens exposed to Solution 2 (0.15 M Na_2SO_4 and 0.5M NaOH) for 1 year is illustrated in Figure 2-4. The affected region extends to a depth about 100 μm and was characterized by loss of mass (increase in porosity, decrease in cohesiveness). The darker gray color in the backscattered images is indicative of either a higher amount of lower atomic number elements. In this chemical system, a higher concentration of sodium than the bulk lighter gray material (altered zone) or an increase in porosity (porous surface zone) or both. The light colored somewhat angular grains in Figure 2-4 are “relic” slag particles. In the unaltered region, many slag particles are unreacted relics surrounded by darker hydration rims. In contrast, the angular particles in the altered zone appear to have been activated by alkali (NaOH) in the immersion solution. In the image below, the hydrated cement (calcium silica hydrate poorly ordered phases) is represented by the medium colored material in the matrix around the slag particles.

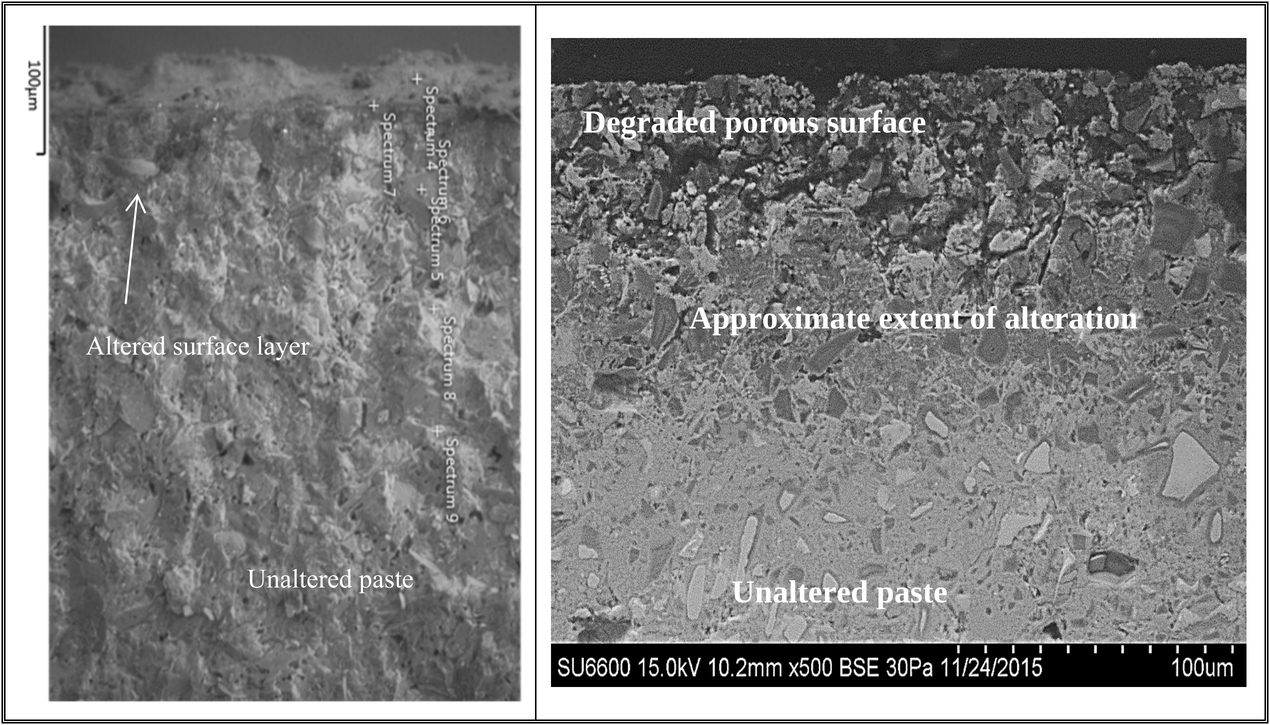

Figure 2-4. PV1S2 after one year exposure. Backscattered image of fractured surface (left) and epoxy impregnated polished surface (right). Note scales of images are different.

The microstructure of the interior region of the PV1 paste sample immersed in Solution 2 (0.15 M Na_2SO_4 and 0.5M NaOH) for one year is illustrated in Figure 2-5. The particles in the matrix include angular light gray slag particles with hydration rims as well as hydrated relic slag particles surrounded by medium gray hydrated Portland cement (hydrated calcium silicate and hydrated calcium aluminate phases). The texture of the surface is consistent with a cohesive material with a few pull-outs that occurred during polishing. The energy dispersive x-ray (EDX) spectra suggest that sulfate and sodium ions from the immersion solution did not penetrate into the sample beyond the zone in which damage was detected (see Figure 2-6). The S and Na in the spectra are proportionally equivalent to values in the blended reagents. The right edge of the photo is a slightly darker gray than the rest of the image and is the transition between the altered surface and unaffected bulk material.

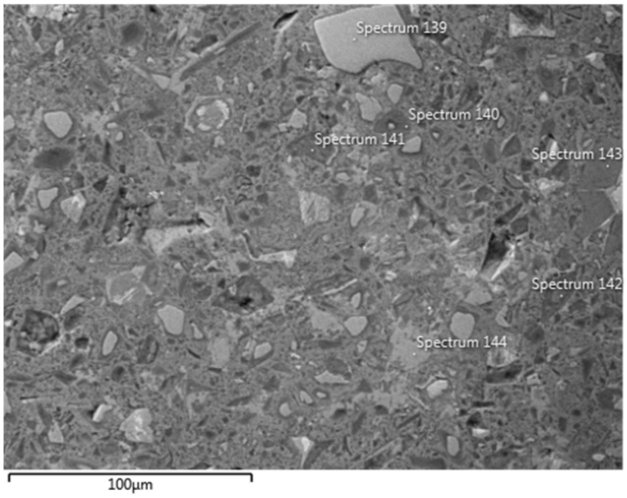

Figure 2-5. Interior of PV1 disk sample exposed to Solution 2 for 1 year.

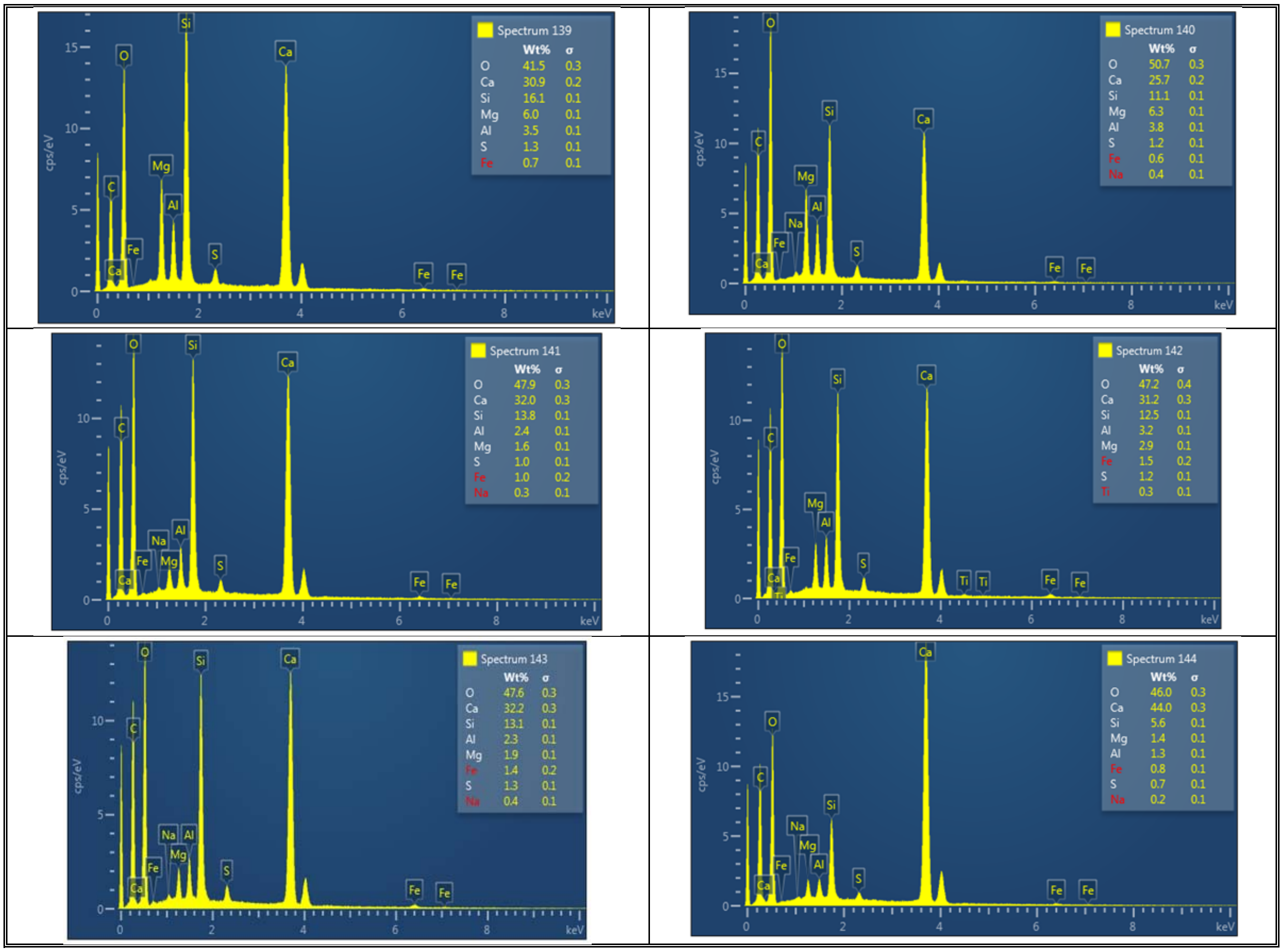

Spectrum 139	Wt%	σ
O	41.5	0.3
Ca	30.9	0.2
Si	16.1	0.1
Mg	6.0	0.1
Al	3.5	0.1
S	1.3	0.1
Fe	0.7	0.1

Spectrum 140	Wt%	σ
O	50.7	0.3
Ca	25.7	0.2
Si	11.1	0.1
Mg	6.3	0.1
Al	3.8	0.1
S	1.2	0.1
Fe	0.6	0.1
Na	0.4	0.1

Spectrum 141	Wt%	σ
O	47.9	0.3
Ca	32.0	0.3
Si	13.8	0.1
Al	2.4	0.1
Mg	1.6	0.1
S	1.0	0.1
Fe	1.0	0.2
Na	0.3	0.1

Spectrum 142	Wt%	σ
O	47.2	0.4
Ca	31.2	0.3
Si	12.5	0.1
Al	3.2	0.1
Mg	2.9	0.1
Fe	1.5	0.2
S	1.2	0.1
Ti	0.3	0.1

Spectrum 143	Wt%	σ
O	47.6	0.3
Ca	32.2	0.3
Si	13.1	0.1
Al	2.3	0.1
Mg	1.9	0.1
Fe	1.4	0.2
S	1.3	0.1
Na	0.4	0.1

Spectrum 144	Wt%	σ
O	46.0	0.3
Ca	44.0	0.3
Si	5.6	0.1
Mg	1.4	0.1
Al	1.3	0.1
Fe	0.8	0.1
S	0.7	0.1
Na	0.2	0.1

Figure 2-6. Energy dispersive x-ray spectra corresponding to locations in Figure 2-5.

Paste 2 Solution 2. The microstructure of the surface of paste PV2 exposed to S2 (0.15 M Na_2SO_4 and 0.5M Na(OH)) for 1 year is illustrated in Figure 2-7. This paste is a quaternary blend of Type V Portland cement, Class F Fly ash, slag cement and silica fume. The image illustrates round medium gray fly ash particles and slag relics with reaction rims. The texture of the surface layer extending at least 65µm into the sample appears to be etched.

The EDX spectra corresponding to the locations marked in Figure 2-7 are provided in Figure 2-8. Decalcification appears to have occurred as the result of immersion in Solution 2 to a depth of at least 50 µm. All locations indicate the presence of higher than background levels of Na which indicates penetration of the immersion solution into this region.

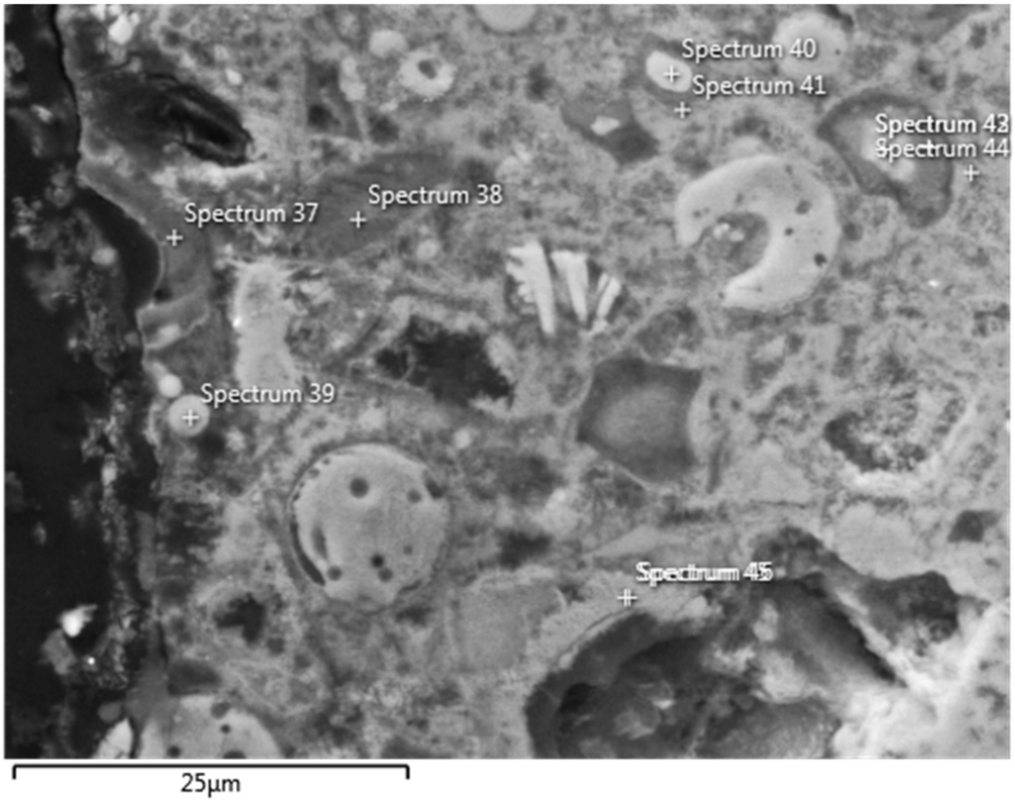

Figure 2-7. PV2S2 paste after one year exposure (Backscattered secondary electron image of epoxy impregnated polished surface).

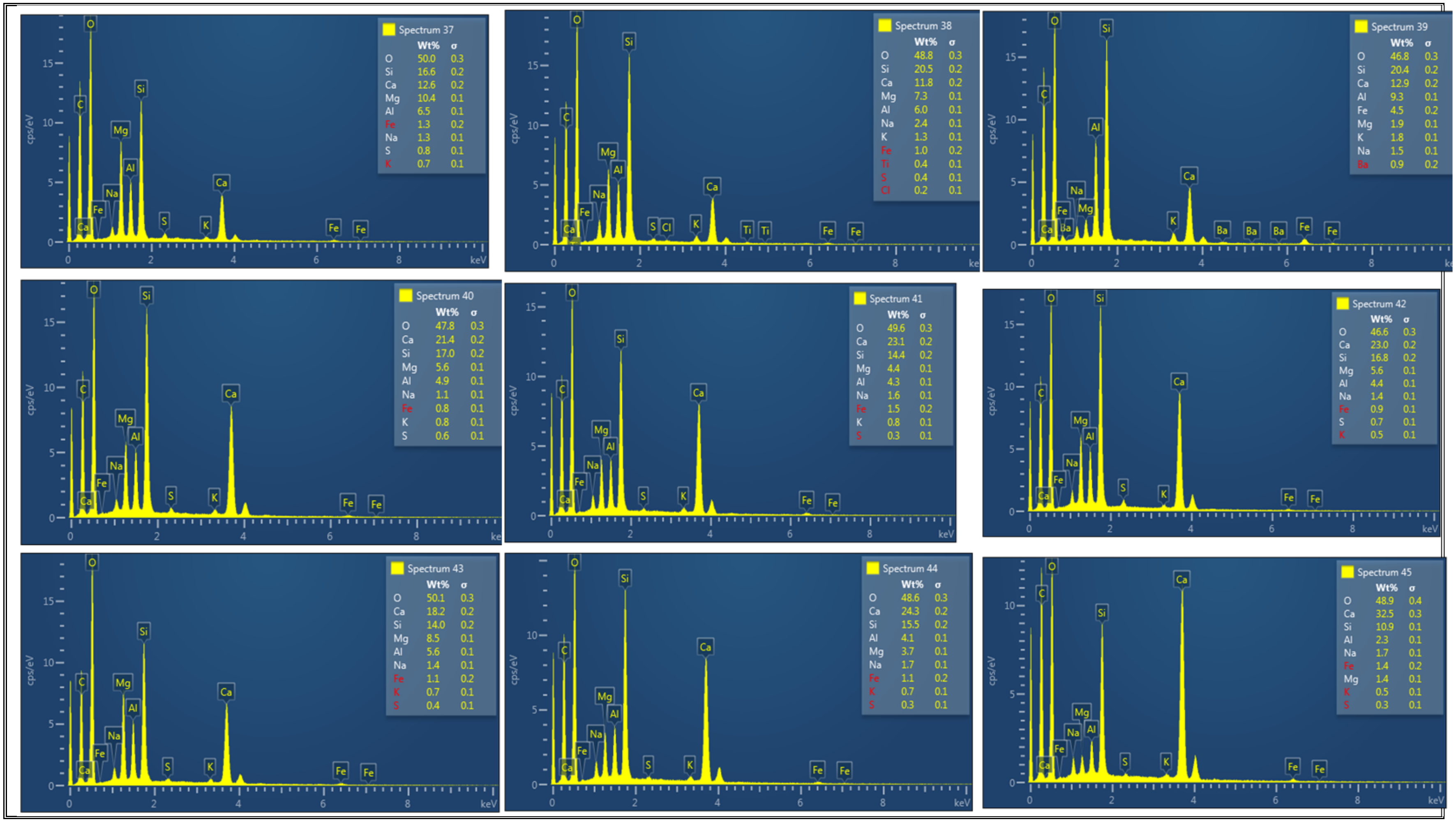

Spectrum 37	Wt%	σ
O	50.0	0.3
Si	16.6	0.2
Ca	12.6	0.2
Mg	10.4	0.1
Al	6.5	0.1
Fe	1.3	0.2
Na	1.3	0.1
S	0.8	0.1
K	0.7	0.1

Spectrum 38	Wt%	σ
O	48.8	0.3
Si	20.5	0.2
Ca	11.8	0.2
Mg	7.3	0.1
Al	6.0	0.1
Na	2.4	0.1
K	1.3	0.1
Fe	1.0	0.2
Ti	0.4	0.1
S	0.4	0.1
Cl	0.2	0.1

Spectrum 39	Wt%	σ
O	46.8	0.3
Si	20.4	0.2
Ca	12.9	0.2
Al	9.3	0.1
Fe	4.5	0.2
Mg	1.9	0.1
K	1.8	0.1
Na	1.5	0.1
Ba	0.9	0.2

Spectrum 40	Wt%	σ
O	47.8	0.3
Ca	21.4	0.2
Si	17.0	0.2
Mg	5.6	0.1
Al	4.9	0.1
Na	1.1	0.1
Fe	0.8	0.1
K	0.8	0.1
S	0.6	0.1

Spectrum 41	Wt%	σ
O	49.6	0.3
Ca	23.1	0.2
Si	14.4	0.2
Mg	4.4	0.1
Al	4.3	0.1
Na	1.6	0.1
Fe	1.5	0.2
K	0.8	0.1
S	0.3	0.1

Spectrum 42	Wt%	σ
O	46.6	0.3
Ca	23.0	0.2
Si	16.8	0.2
Mg	5.6	0.1
Al	4.4	0.1
Na	1.4	0.1
Fe	0.9	0.1
S	0.7	0.1
K	0.5	0.1

Spectrum 43	Wt%	σ
O	50.1	0.3
Ca	18.2	0.2
Si	14.0	0.2
Mg	8.5	0.1
Al	5.6	0.1
Na	1.4	0.1
Fe	1.1	0.2
K	0.7	0.1
S	0.4	0.1

Spectrum 44	Wt%	σ
O	48.6	0.3
Ca	24.3	0.2
Si	15.5	0.2
Al	4.1	0.1
Mg	3.7	0.1
Na	1.7	0.1
Fe	1.1	0.2
K	0.7	0.1
S	0.3	0.1

Spectrum 45	Wt%	σ
O	48.9	0.4
Ca	32.5	0.3
Si	10.9	0.1
Al	2.3	0.1
Na	1.7	0.1
Fe	1.4	0.2
Mg	1.4	0.1
K	0.5	0.1
S	0.3	0.1

Figure 2-8. Elemental spectra corresponding to locations on the polished PVS2 sample in Figure 2-7.

Sample PV2S2 did not display the extent of damage seen in PV2S4. However, PV2S2 did contain spherical features filled with silica gel. These features were detected near the exposed surface in sample PV2S2 and were associated with cracks through the paste. The spheres ranged in size from about 0.05 mm to 1mm and exhibited a variety of morphologies, several of which are illustrated in Figure 2-9. They are filled with silica gel based on EDX spectra. These features are attributed to undispersed agglomerates of silica fume, some if not all of which appear to be participating in chemical degradation via alkali-silica reaction. According to S. Simner, field produced concrete is not expected to contain silica fume agglomerates [16]. Consequently this cause of degradation may be a laboratory phenomenon. Another explanation of these features was proposed by SIMCO Technologies, Inc., i.e., silica gel resulting from ASR of the matrix is deposited in large pores in the paste which were the result of entrapped air bubbles in the paste [8].

The crack in the matrix on the left side of the image in Figure 2-9 was attributed to expansion resulting from ASR, whereas cracks in some of the gel filled features were attributed to post-exposure desiccation. Many more examples of these features were observed in sample PV2S4. Similar features have been described in the literature and attributed to ASR of agglomerated silica fume [4 to 10].

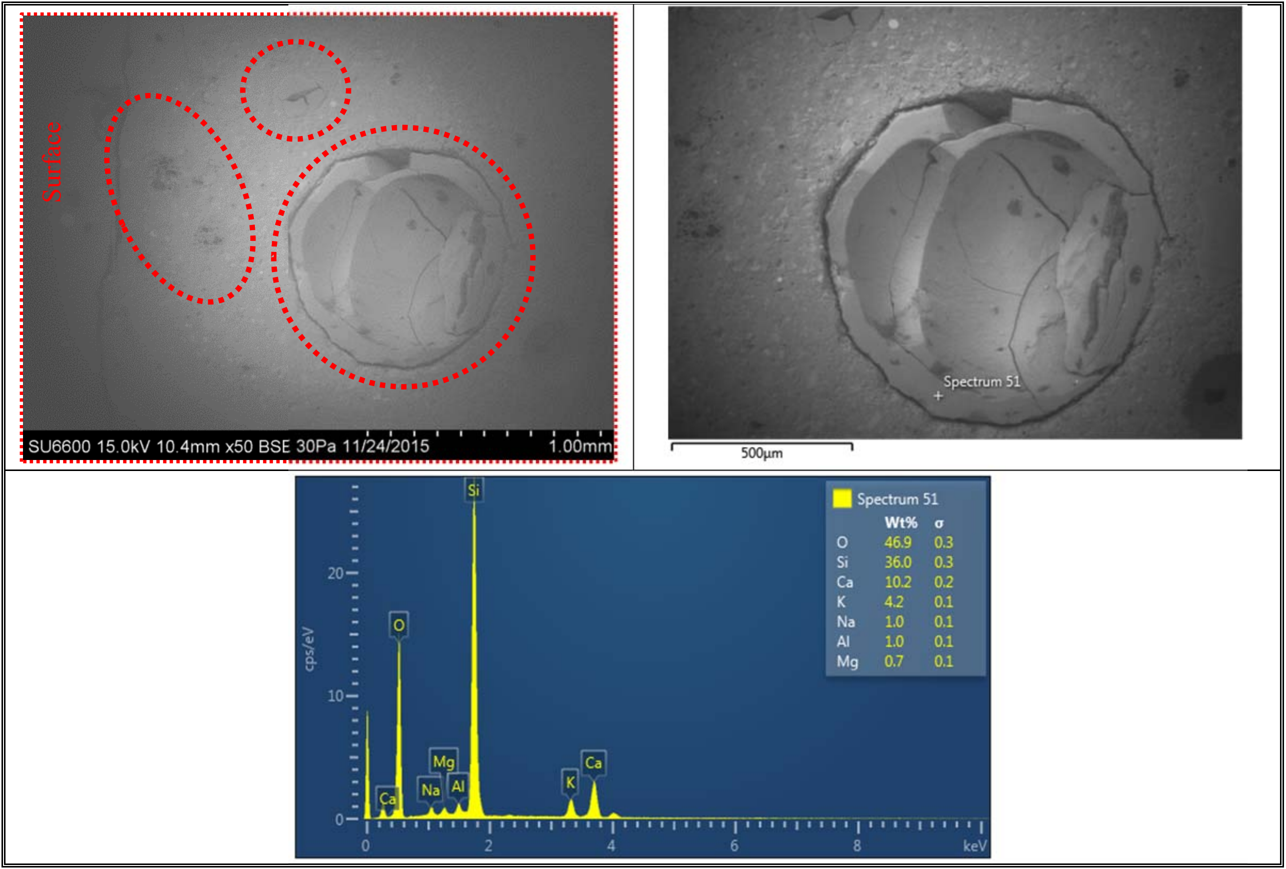

Figure 2-9. Silica gel in pores near surface of PV2S2 polished surface (top); Silica gel composition from EDX spectrum composition (bottom).

Paste 1 Solution 4. The microstructure of a polished surface sectioned perpendicular to the surface of sample PV1immersed in Solution 4 (0.15 M Na_2SO_4, 0.5M NaOH and 3.0 M $NaNO_3$) for 1 year is illustrated in Figure 2-10. This paste is a binary blend of Type I/II Portland cement and GGBFS. The image illustrates an altered / damaged zone about 70 µm thick. The lighter gray particles are unreacted slag grains which in many cases have reaction rims. These particles are dispersed in a matrix of medium gray hydrated Portland cement and hydrated slag with relic textures. Black holes are the result of what appear to be pull-outs of angular grains (unhydrated slag) during the polishing process. The EDX spectra of the areas indicated in the backscattered image suggest some decalcification in the two outlined surface regions (29.0 and 29.4 wt. % Ca) compared to the outlined region about 200 µm from the surface (33.4 wt. % Ca).

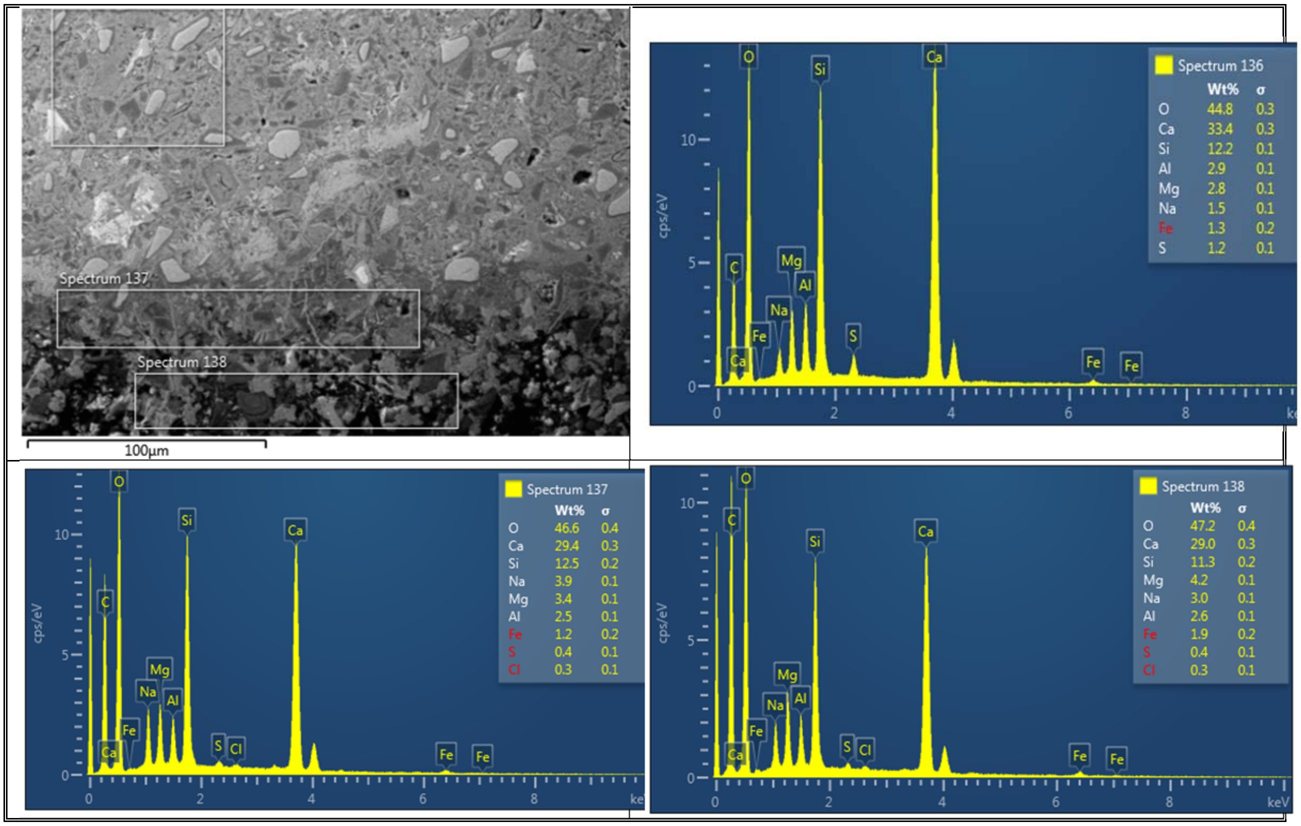

Spectrum 136

	Wt%	σ
O	44.8	0.3
Ca	33.4	0.3
Si	12.2	0.1
Al	2.9	0.1
Mg	2.8	0.1
Na	1.5	0.1
Fe	1.3	0.2
S	1.2	0.1

Spectrum 137

	Wt%	σ
O	46.6	0.4
Ca	29.4	0.3
Si	12.5	0.2
Na	3.9	0.1
Mg	3.4	0.1
Al	2.5	0.1
Fe	1.2	0.2
S	0.4	0.1
Cl	0.3	0.1

Spectrum 138

	Wt%	σ
O	47.2	0.4
Ca	29.0	0.3
Si	11.3	0.2
Mg	4.2	0.1
Na	3.0	0.1
Al	2.6	0.1
Fe	1.9	0.2
S	0.4	0.1
Cl	0.3	0.1

Figure 2-10. Polished epoxy impregnated section of PV1S4.

Paste 2 Solution 4. The microstructure of the surface of quaternary paste PV2 (cement, slag, fly ash and silica fume) immersed in Solution 4 (0.15 M Na_2SO_4, 0.5M NaOH and 3.0 M $NaNO_3$) for 1 year is illustrated in Figure 2-11. The surface of the sample has been severely degraded compared to the other samples discussed, as illustrated by bands of reaction products parallel to the surface.

Large spherical features shown in Figure 2-12 are silica-rich and are assumed to be filled with silica gel. These features were attributed to undispersed silica fume agglomerates. Cracks in the surrounding matrix were attributed to expansion due to alkali silica reaction involving the silica fume agglomerates and alkaline immersion solution. The four images in Figure 2-12 illustrate examples of various expressions of these features, which in sample PV2S4 are usually associated with cracks through. These features are differentiated from fly ash particles which are also round by their large size, association with cracks, and appearance. Fly ash particles in the PV2S4 are illustrated in Figure 2-13. The fly ash particles are typically less than 100 µm in diameter and have a variety of features including various size spheres within spheres and refractory phases such as embedded mullite needles and quartz grains. Surprisingly reaction rims on the fly ash are minimal. An image of the matrix microstructure at a higher magnification is provided in Figure 2-14. The rough texture in this image suggests degradation and weakening of the paste matrix.

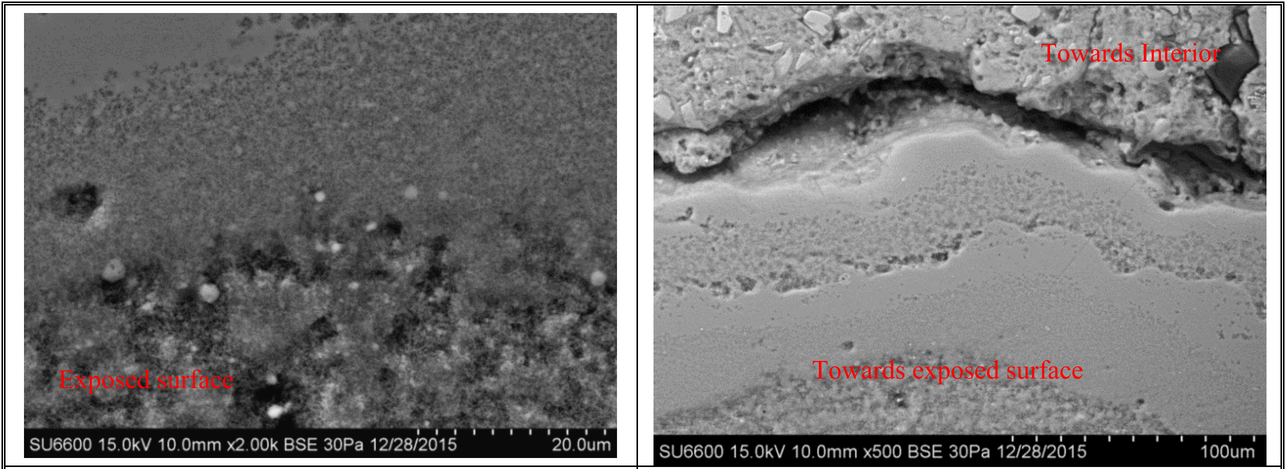

Exposed surface is toward the bottom of photo	Bottom of photo is top of image to left

Figure 2-11. Altered surface of PV2S4 with layering parallel to the surface.

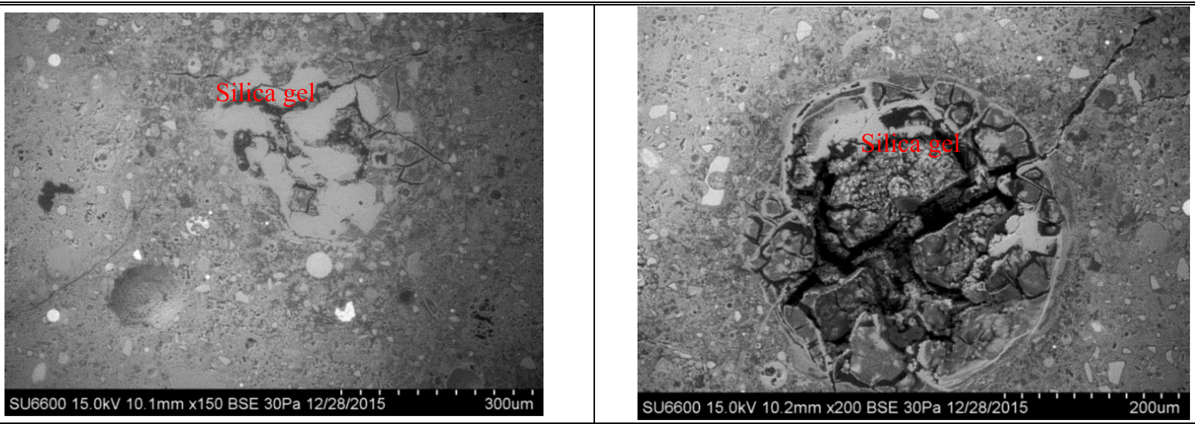

Large silica gel feature with associated cracks, small bright spheres of Fe metal (contaminant in the silica fume from FeSi metal refining). Small round medium gray patricles are fly ash. Dark anuglar particles are slag with hydration rims. Cement hydration products are medium gray and lack particle shape at low magnification	Silica gel feature (possibly silica fume agglomerate) and associated cracking.

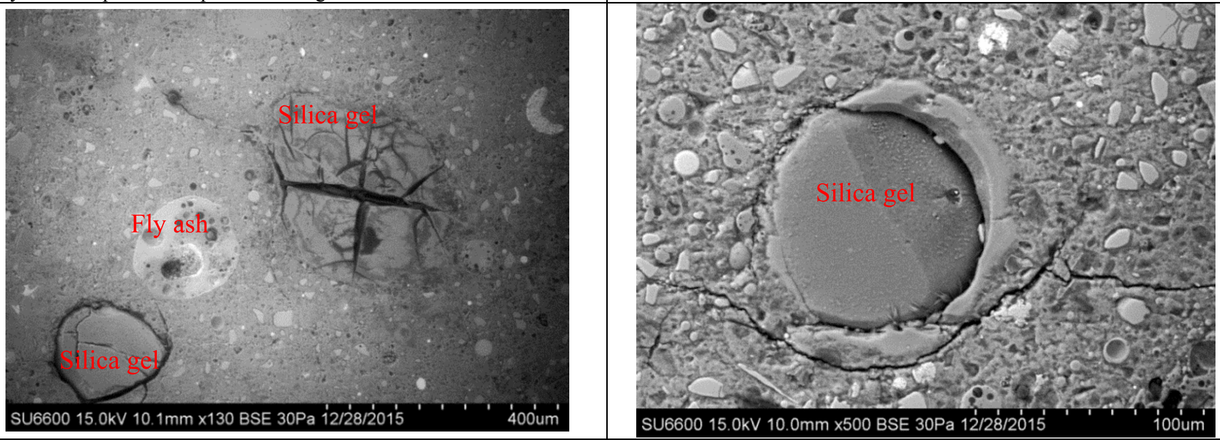

Silica gel features and associated cracking and one large fly ash particle.	Large sphere of silica gel feature, small fly ash spheres and small angular slag particles in a “weak” C-S-H matrix based on rough appearance of the polished surface.

Figure 2-12. Examples of spherical features filled with silica gel. Cracks are indicative of expansion caused by the swelling gel.

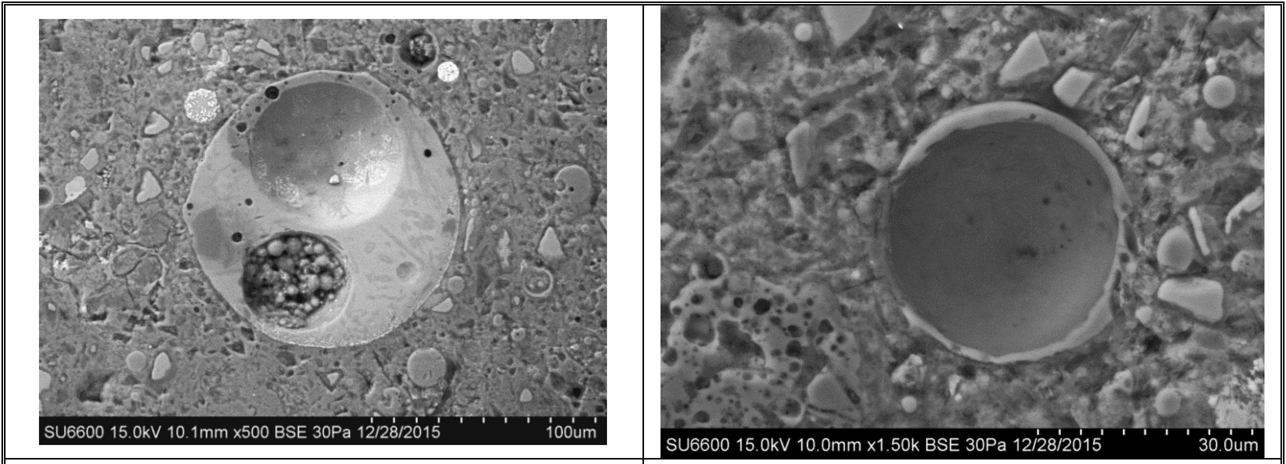

Unreacted fly ash (large sphere in center of image) containing mullite crystals and cenospheres in a matrix that appears corroded.

Hollow fly ash sphere in a corroded matrix as indicated by many pullouts and residual particle boundary etching.

Figure 2-13. Polished epoxy impregnated section of PV2S4.

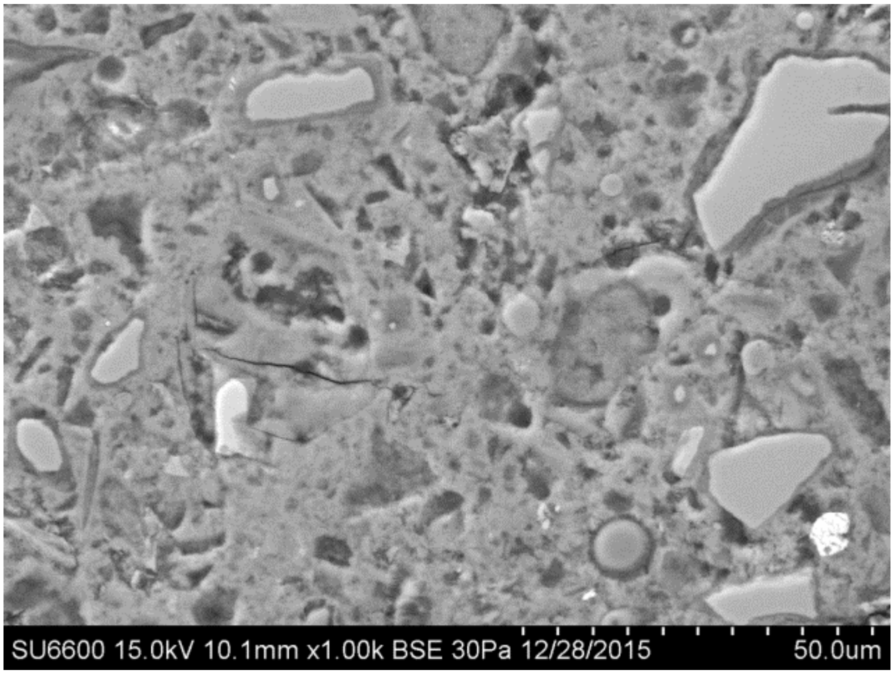

Complex microstructure with many pullouts suggesting a weak matrix. Slag (angular light gray) and fly ash (medium gray).

Figure 2-14. Epoxy impregnated polished surface of interior of PV2S4.

Sample PV2S4 received at SRNL had been cored after immersion and frozen to stop further chemical changes. It was delaminated into thin crumbly layers with the exception of a 3-5 mm core as shown in Figure 2-3. The images in Figure 2-15 were taken from the surface of a delaminated flake recovered from the center of the cutout and about a third of the way from the surface of the as received disk. Based on the EDX spectra and cracking, the material in the images is assumed to be a hygroscopic high sodium (9.5 to 9.7 wt. %) complex cation (Ca ~ 22 to 23 wt. %, Al ~ 5 wt. %, Mg ~ 0.7 to 0.8 wt. %) silica gel. This composition suggests that the entire matrix phase assemblage in PV2, not just silica fume agglomerates, was involved in chemical degradation reactions with the alkali in the immersion solution, S4.

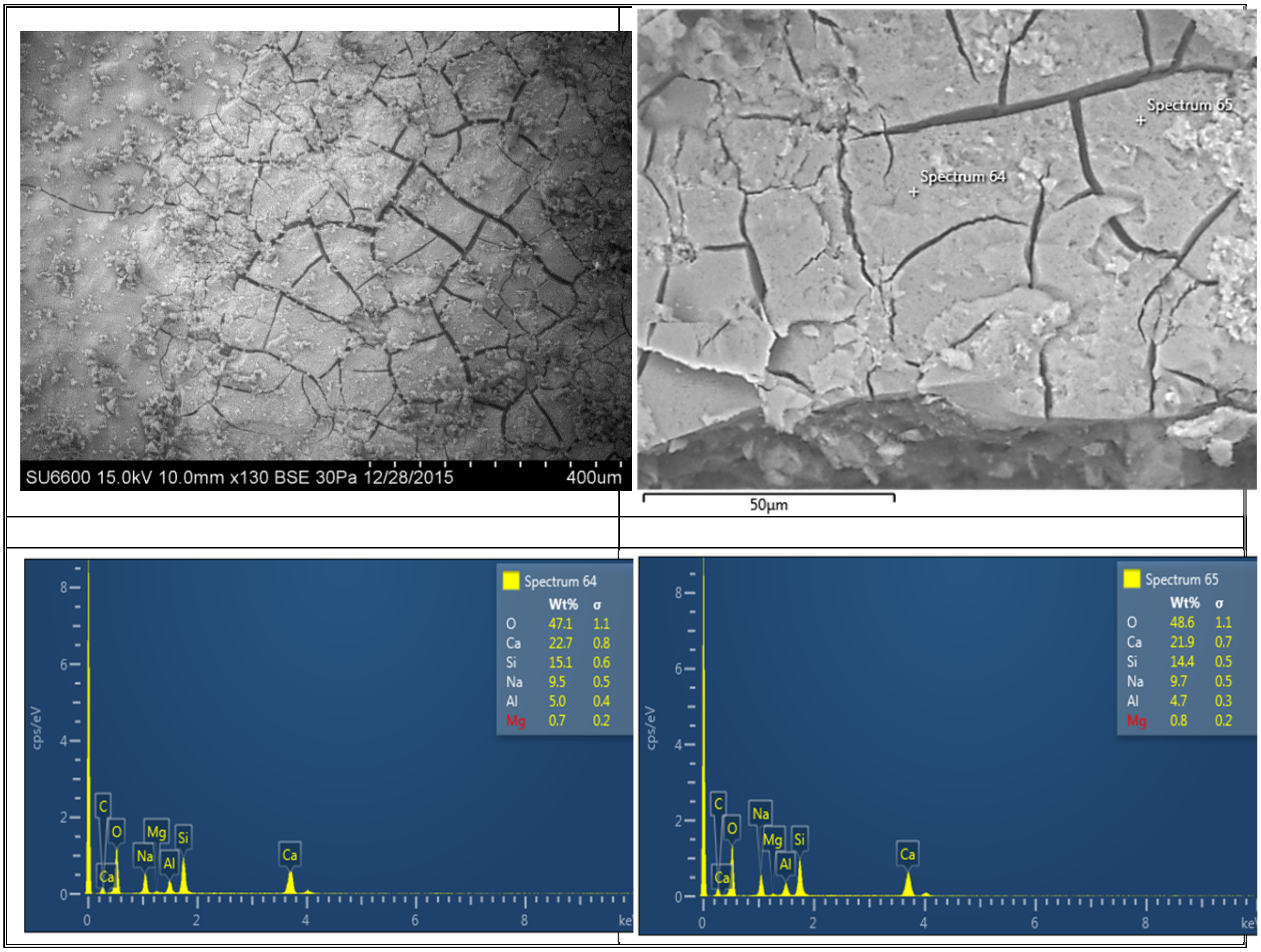

Spectrum 64

	Wt%	σ
O	47.1	1.1
Ca	22.7	0.8
Si	15.1	0.6
Na	9.5	0.5
Al	5.0	0.4
Mg	0.7	0.2

Spectrum 65

	Wt%	σ
O	48.6	1.1
Ca	21.9	0.7
Si	14.4	0.5
Na	9.7	0.5
Al	4.7	0.3
Mg	0.8	0.2

Figure 2-15. Desiccated sodium silicate gel resulting from ASR on the surface of a delaminated flake from the center of sample PV2S4.

The surfaces of some delaminated flakes displayed an additional feature which was tentatively identified as $NaNO_3$ (see Figure 2-16). Similar crystal habits have been previously observed on porous cement samples which have been exposed to salt solutions and then dried. The dendritic phase in these photographs appears to be growing out onto the surface from pores in the sample which is consistent with formation as the result of evaporation. Sodium is present in relatively high concentrations in the spectra which includes underlying material. Nitrogen is not detectable by standard EDX methods used in this evaluation.

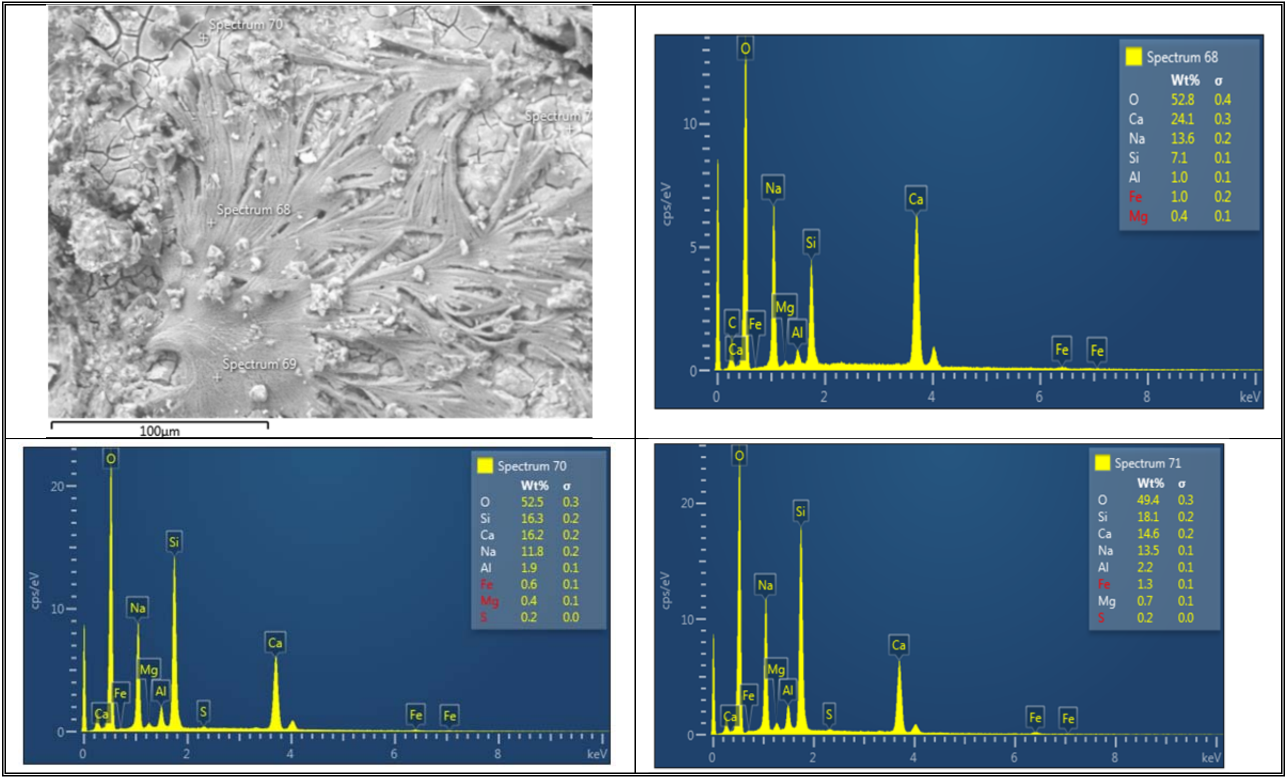

Spectrum 68

	Wt%	σ
O	52.8	0.4
Ca	24.1	0.3
Na	13.6	0.2
Si	7.1	0.1
Al	1.0	0.1
Fe	1.0	0.2
Mg	0.4	0.1

Spectrum 70

	Wt%	σ
O	52.5	0.3
Si	16.3	0.2
Ca	16.2	0.2
Na	11.8	0.2
Al	1.9	0.1
Fe	0.6	0.1
Mg	0.4	0.1
S	0.2	0.0

Spectrum 71

	Wt%	σ
O	49.4	0.3
Si	18.1	0.2
Ca	14.6	0.2
Na	13.5	0.1
Al	2.2	0.1
Fe	1.3	0.1
Mg	0.7	0.1
S	0.2	0.0

Figure 2-16. Dendritic phase formed on the surface of flakes from PV2S4 after formation of underlying silica gel, which showed cracks attributed to drying shrinkage.

2.3 Mineralogy

Phases identified in x-ray diffraction powder patters of samples PV1S2, PV2S4, PV2S2 and PV2S4 are summarized and tabulated in Table 2-1.

The phases identified in PV1 immersed in Solutions 2 and 4 were similar and typical of a hydrated binary paste containing a 60:40 blend of Portland cement (Type I/II or V) and GGBFS [7]. The same phase assemblages were identified for material collected from the top, middle, and bottoms of these samples. The only exception was that sodium nitrate was identified in the patterns for PV1S4, top and middle. Solution 4 contained 3.0 M $NaNO_3$ in addition to Na(OH) and Na_2SO_4. Gypsum, an indicator of sulfate attack, was not identified in paste PV1immersed in Solution 2 and Solution 4, both of which contained 0.15M Na_2SO_4 and 0.5 M NaOH. Ettringite, a calcium aluminate sulfate hydrate was present throughout the PV1 samples exposed to both Solutions 2 and 4. According to calculation by SIMCO Technologies, Inc. personnel, there is not enough sulfur in this mix for ettringite to be present in cured samples. Consequently, it is most likely the result of exposure to sulfate in the exposure solutions, which has migrated into the samples and reacted to form this phase [3]. X-ray diffraction patterns do not allow differentiation between ettringite formed from normal hydration of Portland cement and ettringite formed as the result of sulfate ingress.

Some of the phases identified in a sample taken from the center of PV2 exposed to Solution 2 are those that would be expected from a quaternary blend of cement, GGBFS, Class F fly ash, and silica fume. Poorly ordered CSH hydrates (C-S-H gel) were present in samples taken from the surface, below the delaminating surface layer, and center. Quartz and mullite are residual refractory phases from the fly ash. However, the presence of gypsum throughout the sample of PV2 immersed in Solution 2 suggests the

Table 2-1. Summary of phases identified in x-ray diffraction powder patterns

Phase	PV1S2 Top, middle, bottom (same pattern)	PV1S4 Top and middle	PV2S2 Surface w/o grinding	PV2S2 Under surface w/o grinding	PV2S2 Center	PV2S4 Top surface	PV2S4 Under surface layer	PV2S4 Center
Hydrated paste phases								
Portlandite $Ca(OH)_2$	x	x	--	x	x	x	x	x
$Ca_2SiO_4xH_2O$ Pattern 011-0211	x	x	--	x	--	x	--	x
Hydrocalumite (layered double hydroxide$(M^{2+})_{1-x}$ $(M^{3+})_x(OH)_2(Anion^{n-})_{x/n}yH_2O$	x	x	--	--	--	x	x	x
Ettringite (also possible reaction product) $Ca_6Al_2(SO_4)_3(OH)_{12}\cdot 26H_2O$	x	x	--	--	x	x	x	x
Heulandite (zeolite) $(Ca,Na)_{2-3}Al_3(Al,Si)_2Si_{13}O_{36}\bullet 12(H_2O)$	x	x	--	--	--	--	--	--
Poorly ordered calcium silicate hydrate (C-S-H) centered at about 30° 2Θ	x	x	x	x	x	x	x	x
Residual unreacted phases								
$CaSiO_4$ Larnite (residual cement)	x	x	--	--	--	--	--	--
Amorphous silicate (Unreacted slag (30° 2Θ)	Based on SEM overlap with hydrated silicate	Based on SEM overlap with hydrated silicate	Based on SEM overlap with hydrated silicate	Based on SEM overlap with hydrated silicate	Based on SEM overlap with hydrated silicate	Based on SEM overlap with hydrated silicate	Based on SEM overlap with hydrated silicate	Based on SEM overlap with hydrated silicate
Mullite $Al_6Si_2O_{13}$ Refractory phases in fly ash	--	--	x	x ground sample	x	x	x	x
Quartz SiO_2 Refractory phases in fly ash	--	--	x	x ground sample	x	x	x	x
Corrosion products from reaction with immersion solutions								
Gypsum $CaSO_42H_2O$	--	--	x	x ground sample	x	--	--	--
Pooly ordered phase silicate gel between 10-25 2Θ)	--	--	x	x	x	x?	x	x
Post immersion phases resulting from carbonation and/or drying								
Calcite $CaCO_3$	--	x	x	x	x	x	--	--
Vaterite $CaCO_3$	--	--	x ground sample	--	x	--	--	--
Gaylussite $(Na_2,Ca)(CO_3)_2\cdot 5H_2O$	--	--	x	x	--	--	--	--
Nitratine $NaNO_3$	--	x	--	--	--	--	x	x

onset of sulfate attack and weakening of the matrix. Ettringite was not identified in the surface or near surface subsamples but was identified in the center of PV2S2.

A poorly ordered silicate phases was detected on the surface and to a lesser extent throughout the sample. This amorphous material was assumed to be silica gel resulting from alkali silica reaction. In addition to calcite, vaterite, a $CaCO_3$ polymorph, and gaylussite, $(Na_2,Ca)(CO_3)_2 \cdot 5H_2O$, were detected in this sample. The timing of carbonation was post immersion because the immersion solution did not contain carbonate. Carbonation throughout the sample suggests higher porosity compared to PV1 immersed in Solution 2.

Some of the phases identified in sample PV2S4 were similar to those expected from the quaternary blend. A poorly ordered phase identified in sample PV2S4 was attributed to silica gel. In addition, sodium nitrate was identified throughout the sample.

3.0 DISCUSSION

Visual examination of the four paste samples prepared by SIMCO Technologies, Inc. which were sent to SRNL for additional characterization indicates that the PV1 samples immersed in Solution 2 (0.15 M Na_2SO_4 and 0.5M NaOH) and Solution 4 (0.15 M Na_2SO_4, 0.5 M NaOH, and 3.0 M $NaNO_3$) showed minimal alteration of the surface exposed to the immersion solutions. The macroscopic appearance of the PV2 samples exposed to Solutions 2 and 4 indicated significant degradation. The damage in PV2S4 was more extensive than the damage observed in PV2S2.

The PV2 samples immersed in Solutions 2 and 4 contained features that were interpreted as silica fume agglomerates that reacted with high pH alkaline solutions to form silica gel. These features were often associated with cracks. Similar features have been described in the literature and attributed to ASR of agglomerated silica fume [4 to 10]. An alternative interpretation is that these features are pores (air bubbles from mixing and casting) partially filled or filled with silica gel. PV2S4 also displayed delaminated layers and extensive cracking on the surface and interior of the sample. Silica gel presumably resulting from ASR was observed on the cracked surfaces which were perpendicular to the short axis of the disk shaped sample.

Portland cement concrete exposed to alkali hydroxides ions can experience a form of chemical degradation in which the alkali hydroxide reacts with siliceous aggregates (poorly crystalline, weathered, or strained siliceous aggregates are most susceptible) to form a hygroscopic silica gel which is expansive in the presence of water. The reaction between the alkali hydroxide and reactive silicate results in a water soluble alkali silicate, which has a strong tendency to attract moisture from the hardened paste. The source of the alkali can be internal (in the cement itself) or external (sulfate ingress). In concrete, the gel typically forms at the paste-reactive aggregate interface and in fractures in the aggregate and is expansive. The expansion causes cracking which results in spalling of the surface (external source of alkali) or damage throughout the entire concrete element (internal source of alkali).

In the paste samples characterized in this study, the source of the reactive silicate phase(s) must be one or more components in the paste itself because the samples did not contain any aggregates. The specific paste ingredient(s) involved in the increased susceptibility of the quaternary PV2 paste was/were not identified. The source of sodium hydroxide was the immersion solution. SEM imaging indicated that a considerable amount of slag and fly ash remained as residual material in the PV1 and PV2 pastes exposed to both Solutions 2 and 4. The slag particles were surrounded by hydration products with no associated cracking. The fly ash particles in the PV1 and PV2 samples did not appear to have thick reaction rims or to be pitted or otherwise corroded. It is interesting that larnite, Ca_2SiO_4, a residual cement phase, was

identified in the PV1S2 and PV1S4 paste but was not identified in the PV2S2 and PV2S4 pastes which experienced the most damage
Over the time frame of this study, GGBFS, GGBFS hydration phases, and fly ash either do not appear to be susceptible to ASR or do not result in expansion during the time frames studies. Damage was not observed in PV1 samples exposed to Solutions 1 or 2.

The role of curing time and conditions prior to immersion testing of the paste samples was not evaluated. Longer curing times in saturated $Ca(OH)_2$ solution or 100 % relative humidity are expected to increase slag hydration and fly ash pozzolanic reactions and thereby change the chemical and physical properties of these paste samples.

Sulfate attack is also indicated in the PV2S2 sample (gypsum) and PV2S4 (ettringite). The presence of gypsum is an early indicator of sulfate attack. In addition, PV2S4 contained $NaNO_3$ throughout the entire sample. Immersion Solution 4 which contained 3.0 M $NaNO_3$ provided a large concentration gradient and driving force for ingress of the sodium salts into the paste samples. Crystallization of $NaNO_3$ as the result of drying of the samples after they were removed from the immersion solutions is assumed to have enhanced delamination degradation of sample PV2S4.

It is worth noting, that neat Portland cement Type I/II paste and neat Portland cement Type V paste samples immersed in Solutions 2 and 4 had negligible damage after one year immersion based on visual examination of photos provided by SIMCO Technologies, Inc. The Type V (high sulfate resistant cement) did not provide a benefit with respect to overall damage because mechanisms other than sulfate attack, i.e., alkali silica reaction, and soluble salt ($NaNO_3$) crystallization contributed to the degradation.

Both the PV1 and PV2 samples contained a significant amount of unreacted slag and the PV2 samples contained unreacted fly ash. Longer curing times (> 6 months) at 100 % RH or in lime water prior to immersion in the caustic, sodium salt solutions are expected to result in samples that are more hydrated and therefore more resistant to chemical degradation. In addition the pastes with high $CaO + MgO / SiO_2 + Al_2O_3$ mass ratios appear to be more resistant to decalcification and subsequent degradation than pastes with low ratios. Evidence for this is the appearance of the neat Type I/II and neat Type V cement paste samples with ratios of 2.6 and 2.7 and the PV1 paste (ratio of 1.7) compared to PV2 paste (ratio of 0.8) after exposure to Solutions 2 and 4 for 1 year. See Table 3-1 for a comparison of the normalized major oxide ratios of these pastes.

Table 3-1. Normalized major oxide composition of PV1 and PV2 pastes and Type 1/II and Type V pastes.

Oxides	**PV1 Binder**	**PV2 Binder**	**PV1b Type I/II Cement Paste**	**PV2b Type V Cement Paste**
SiO_2	0.288	0.421	0.214	0.215
Al_2O_3	0.060	0.109	0.049	0.039
CaO	0.551	0.351	0.665	0.652
MgO	0.056	0.060	0.011	0.027
Mass fraction	0.954	0.942	0.939	0.932
CaO / SiO_2	**1.9**	**0.8**	**3.1**	**3.0**
$(CaO + MgO) / (SiO_2 + Al_2O_3)$	**1.7**	**0.8**	**2.6**	**2.7**

4.0 CONCLUSION

The potential for chemical degradation of the Saltstone Disposal Units (SDU) concretes resulting from exposure to highly alkaline sodium salt solutions was investigated. The samples analyzed in this study were cement pastes prepared in the SIMCO Technologies, Inc. concrete laboratory by SIMCO personnel. They were based on the paste fractions of the concretes used to construct the Saltstone Disposal Units (SDUs). SDU 1 and 4 concrete pastes were represented by the PV1 test specimens. The paste in the SDU 2, 3, 5, and 6 concrete was represented by the PV2 test specimens. The pastes were cured for 56 days in curing chamber and then exposed to aggressive solutions. SIMCO Technologies, Inc. selected the chemicals and proportions in the aggressive solutions to approximate proportions in the saltstone pore solution [2, 3, 5, and 6].

After exposure, the samples were frozen to prevent additional chemical transport. Selected archived (retrieved from the freezer) samples were sent to the Savannah River National Laboratory (SRNL) for additional characterization using x-ray diffraction (XRD), scanning electron microscopy (SEM), and energy dispersive x-ray (EDX) spectroscopy. Characterization results are summarized in this report. In addition, a correlation between the oxide composition of the pastes and their chemical durability in the alkaline salt solutions is provided.

It is important to understand that the materials utilized in the exposure testing are not completely representative of the SDU6 concrete in that: (1) they contain no sand or aggregate, (2) the lack of aggregate can impact the de-agglomeration and dispersion of components, such as silica fume, during mixing, and (3) pre-exposure curing time (56 days at 100 % relative humidity) was significantly less than would be anticipated in the field. Additionally, SDU concrete in the field will be predominantly in contact with cured saltstone rather than immersed in saltstone pore solutions.

The SIMCO Technologies, Inc. test protocol can be considered an accelerated method for evaluating the potential for concrete degradation. Immersion testing of the concrete paste samples in simulant pore solution provides an essentially infinite supply of aggressive chemical species and water for formation of hydrated reactions products and through which the chemicals are transported into the paste samples. Also it should be noted that the paste fraction makes up about 20 volume percent of the actual concrete so the expression of damage in paste samples is not expected to be the same as that for concrete which contains about 80 volume percent non porous quartz sand and granite aggregate. A complete description of the SIMCO Technologies Inc., test program funded by the Cementitious Barriers Partnership is provided elsewhere [2, 4, and 5].

Alteration / degradation of PV1 paste samples (corresponding to the paste in SDU 1 and 4 concrete) immersed in Solutions 2 (0.15 M Na_2SO_4 and 0.5M NaOH) and 4 (0.15 M Na_2SO_4, 0.5M NaOH and 3.0 M $NaNO_3$) for one year was limited to a depth of less than about 100 µm. This was also the case for samples made with 100 % Portland Type I/II cement (PV1b) and 100 % Portland cement type V (PV2b). On the other hand, the PV2 paste samples immersed in Solutions 2 and 4 for one year were severely degraded, i.e, cracked. The sample immersed in Solution 4 was more degraded than the one exposed to Solution 2.

The cracks in the PV2 samples were attributed to expansion caused by alkali silica reaction (ASR) of the silica fume agglomerates in the paste itself. Ettringite was observed in these samples but did not appear to be the cause of cracking. Although sodium nitrate is not usually associated with chemical alteration of cement paste or concrete, the presence of high concentrations of sodium nitrate (3.0 M $NaNO_3$) in Solution 4 seemed to accentuate the extent of degradation of the paste samples. Salt precipitation on crack surfaces and along planes of weakness caused by expansion resulted in what appears to be physical salt attack. Further testing is required to evaluate whether this effect is a chemical or physical phenomena, or a combination of both.

The samples examined in this evaluation were cured in sealed containers for only 56 days prior to immersion in the aggressive alkaline salt solutions. If the samples had been cured for a longer time at 100 % relative humidity or in saturated lime water (months to years), they would be more mature, i.e, more portlandite would have reacted with the silica fume agglomerates and fly ash prior to exposure to aggressive chemicals. Portlandite was present in all exposed samples thereby supporting the idea that longer curing times under moist conditions may result in additional hydration and pozzolanic reactions and hence improved resistance to chemical attack.

The bulk oxide composition of concrete paste was identified as an important parameter in understanding chemical degradation and durability. The effect of pozzolans and other supplemental cementitious materials on bulk oxide composition should be evaluated for unusual exposure environments. Higher $(CaO + MgO) / (SiO_2 + Al_2O_3)$ resulted in better chemical durability in highly alkaline environments typical of legacy salt waste solutions and cement waste forms.

Conditions encountered in radioactive waste disposal scenarios can be significantly different than conditions on which engineering codes and standards are based. Durability of concrete and other cementitious materials must be evaluated for chemical environments expected in the disposal setting.

5.0 REFERENCES

1. Simco Technologies, Inc. 2009. “Report -Tasks 2 and 4. Experimental Results from Vault Concretes”, SRNL-STI-2008-00050 Rev. 1, Attachment 3, Subcontract AC48992N, report for Washington Savannah River Company, Aiken, SC 29808.

2. Protiere, Y. and E. Samson, 2015. “Cementitious Barriers Partnership, Task 12 – Experimental Study, OPC Paste Samples Exposed to Aggressive Solutions” CBP-TR-2015-001-Rev. 0, report for Cementitious Barriers Partnership submitted to the Savannah River National Laboratory, Aiken, SC 29808 and CRESP/Vanderbilt University, TN, 37235, SIMCO Technologies Inc. contract manager.

3. SIMCO Technologies, Inc., 2009. “Saltstone Matrix Characterization and Stadium Simulation Results”, SIMCO Technologies Inc., Task 6 Report Subcontract SIMCORD08009, AC48992N, SRNS-STI-2009-00477 Rev. 0, report for Cementitious Barriers Partnership submitted to the Savannah River National Laboratory, Aiken, SC 29808.

4. Protiere, Y. and E. Samson, 2015. “Cementitious Barriers Partnership Concrete Mixture Characterization”, CBP-TR-2015-008, Rev. 0, report for Cementitious Barriers Partnership submitted to the Savannah River National Laboratory, Aiken, SC 29808 and CRESP/Vanderbilt University, TN, 37235, SIMCO Technologies Inc. contract manager.

5. Protiere, Y. and E. Samson, 2015. “Cementitious Barriers Partnership Task 12 – Experimental Study, SCM Paste Samples Exposed to Aggressive Solutions”, CBP-TR-2015-007, Rev. 1, submitted to the Savannah River National Laboratory, Aiken, SC 29808 and CRESP/Vanderbilt University, TN, 37235, SIMCO Technologies Inc. contract manager.

6. SIMCO Technologies, Inc., 2010. “Saltstone Characterization and Parameters for Performance Assessment Modeling”, SRNL-STI-2010-00515, Rev. 0, Task 6 Report Update, Subcontract SIMCORD08009, AC48992N, report for Savannah River Nuclear Solutions, Aiken, SC 29808.

7. Langton, C. A., and D. M. Missimer, 2014. “X-ray Diffraction of Slag-based Sodium Salt Waste Forms”, CBP-TR-2014-04, Rev. 0 and SRNL-STI-2014-00397, Rev. 1, Savannah River National Laboratory, Aiken, SC, 29808.

8. Samson, E. 2016. Personal communication with C. A. Langton, Savannah River National Laboratory, Aiken SC 29808.

9. Lagerbald, B. and P. Utkin, 1995. “Undispersed granulated Silica Fume in Concrete – Chemical System and Durability Problems”, Mat. Res. Soc. Symp. Proc. V.370. Boston, MA.

10. Hooton, R.D., R.F. Bleszynski, A. Boddy, 1998. “Issues related to silica fume dispersion in concrete”, The Sidney Diamond Symposium, American Ceramic Society, Westerville, OH, p. 435-446.

11. Marusin, S.L. and L.B. Sockwell, 2000. “Alkali-silica reaction in concrete caused by densified silica fume lumps: a case study,” Cem. Concr. Aggreg., v.22(2), p. 90-94.

12. Rangaraju, P. and Olek, J., 2000. "Evaluation of the Potential of Densified Silica Fume to Cause Alkali-Silica Reaction in Cementitious Matrices Using a Modified ASTM C 1260 Test Procedure," Cem. Con. and Aggre., v. 22(2), pp. 150-159

13. Juenger, M.C.G. and C.P. Ostertag, 2004. "Alkali-silica reactivity of large silica fume-derived particles", Cement and Concrete Research, v. 34, p. 1389-1402.

14. Diamond, S. S. Sadananda, and N. Thaulow, 2004. "Reaction products of densified silica fume agglomerates in concrete", v. 34, p. 1625-1632.

15. Maas, A.J., Ideker, J.H., and Juenger, M.C.G, 2006. "Alkali silica reactivity of agglomerated silica fume", Cem. Con. Res. V.37, p. 166-174.

16. Simner, S.P., July 22, 2016. Review comment on report SRNL-STI-2016.00214, Savannah River N, Aiken SC 29808.

ATTACHMENT 1. X-ray Diffraction Patterns for Samples PV1S2, PV1S4, PV2S2, and PV2S4

PV1S2

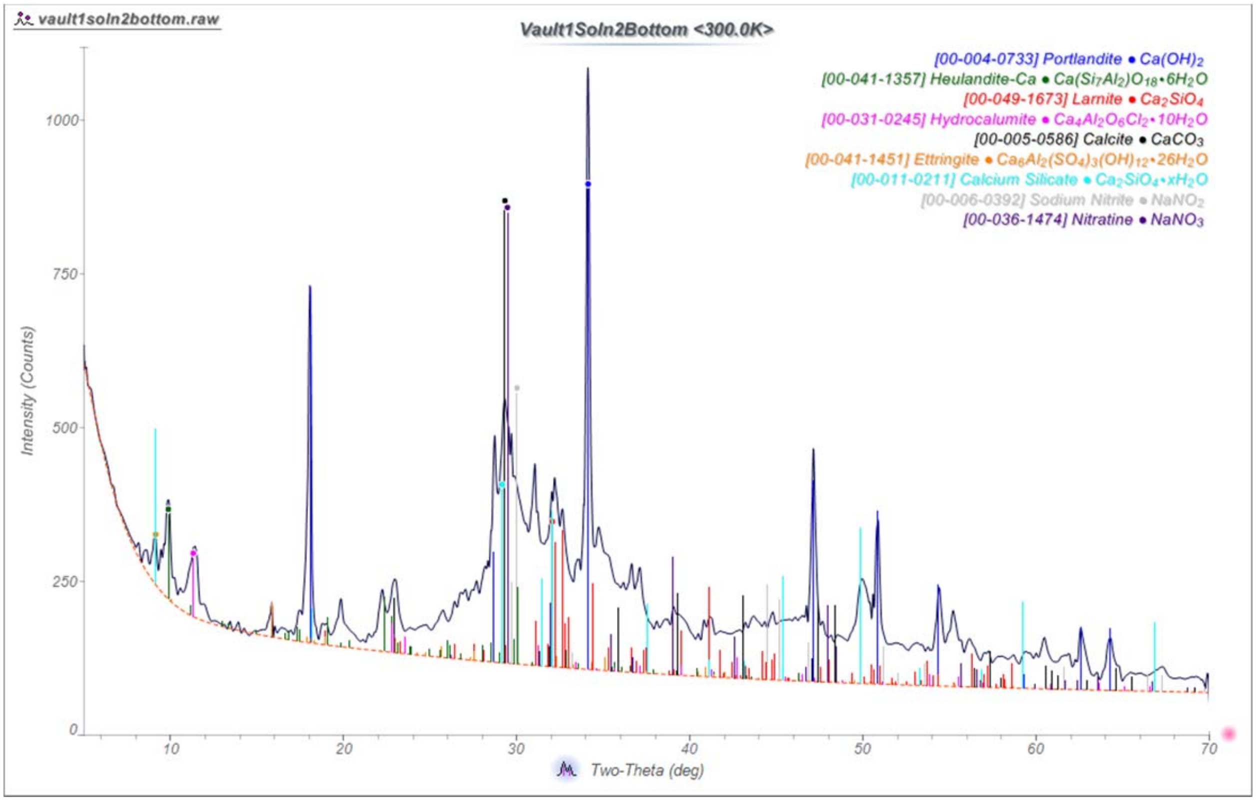
vault1soln2bottom.raw
Vault1Soln2Bottom <300.0K>
[00-004-0733] Portlandite • $Ca(OH)_2$
[00-041-1357] Heulandite-Ca • $Ca(Si_7Al_2)O_{18}•6H_2O$
[00-049-1673] Larnite • Ca_2SiO_4
[00-031-0245] Hydrocalumite • $Ca_4Al_2O_6Cl_2•10H_2O$
[00-005-0586] Calcite • $CaCO_3$
[00-041-1451] Ettringite • $Ca_6Al_2(SO_4)_3(OH)_{12}•26H_2O$
[00-011-0211] Calcium Silicate • $Ca_2SiO_4•xH_2O$
[00-006-0392] Sodium Nitrite • $NaNO_2$
[00-036-1474] Nitratine • $NaNO_3$
Intensity (Counts)
0
250
500
750
1000
10
20
30
40
50
60
70
Two-Theta (deg)

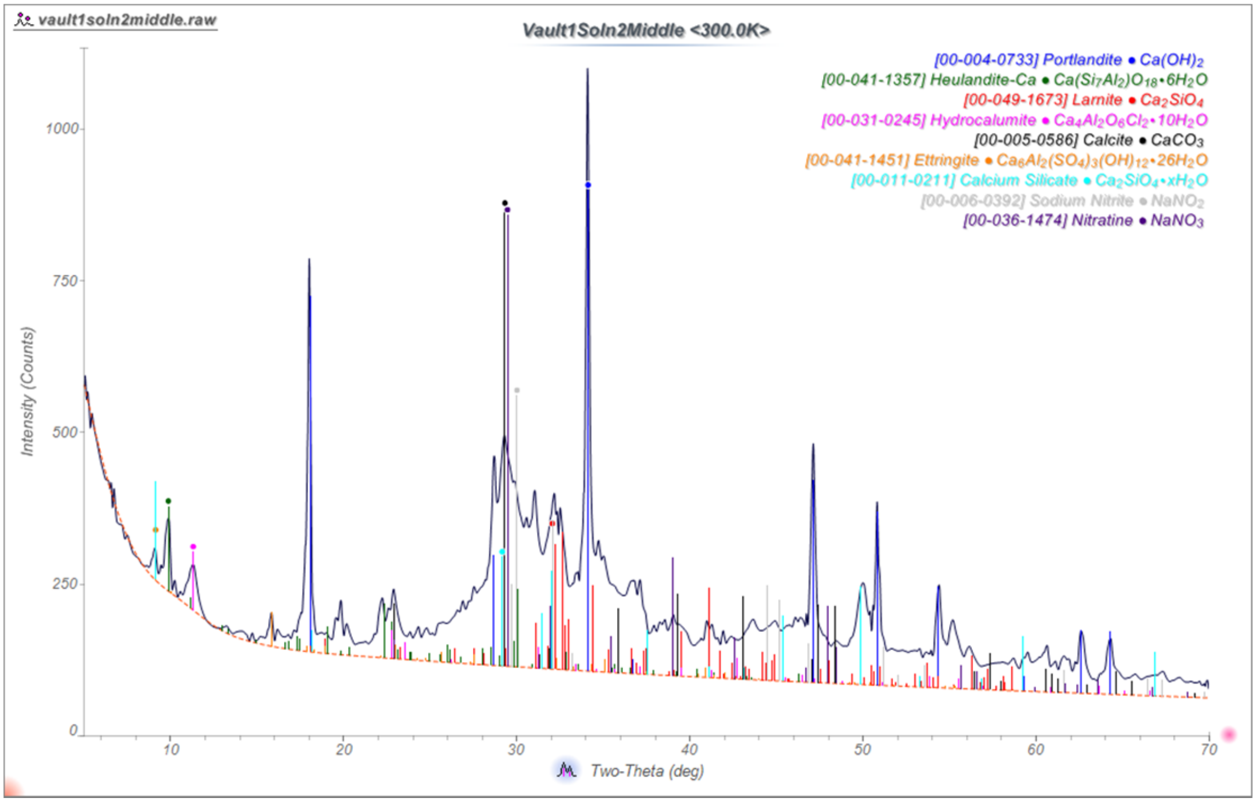
vault1soln2middle.raw
Vault1Soln2Middle <300.0K>
[00-004-0733] Portlandite • $Ca(OH)_2$
[00-041-1357] Heulandite-Ca • $Ca(Si_7Al_2)O_{18}•6H_2O$
[00-049-1673] Larnite • Ca_2SiO_4
[00-031-0245] Hydrocalumite • $Ca_4Al_2O_6Cl_2•10H_2O$
[00-005-0586] Calcite • $CaCO_3$
[00-041-1451] Ettringite • $Ca_6Al_2(SO_4)_3(OH)_{12}•26H_2O$
[00-011-0211] Calcium Silicate • $Ca_2SiO_4•xH_2O$
[00-006-0392] Sodium Nitrite • $NaNO_2$
[00-036-1474] Nitratine • $NaNO_3$
Intensity (Counts)
0
250
500
750
1000
10
20
30
40
50
60
70
Two-Theta (deg)

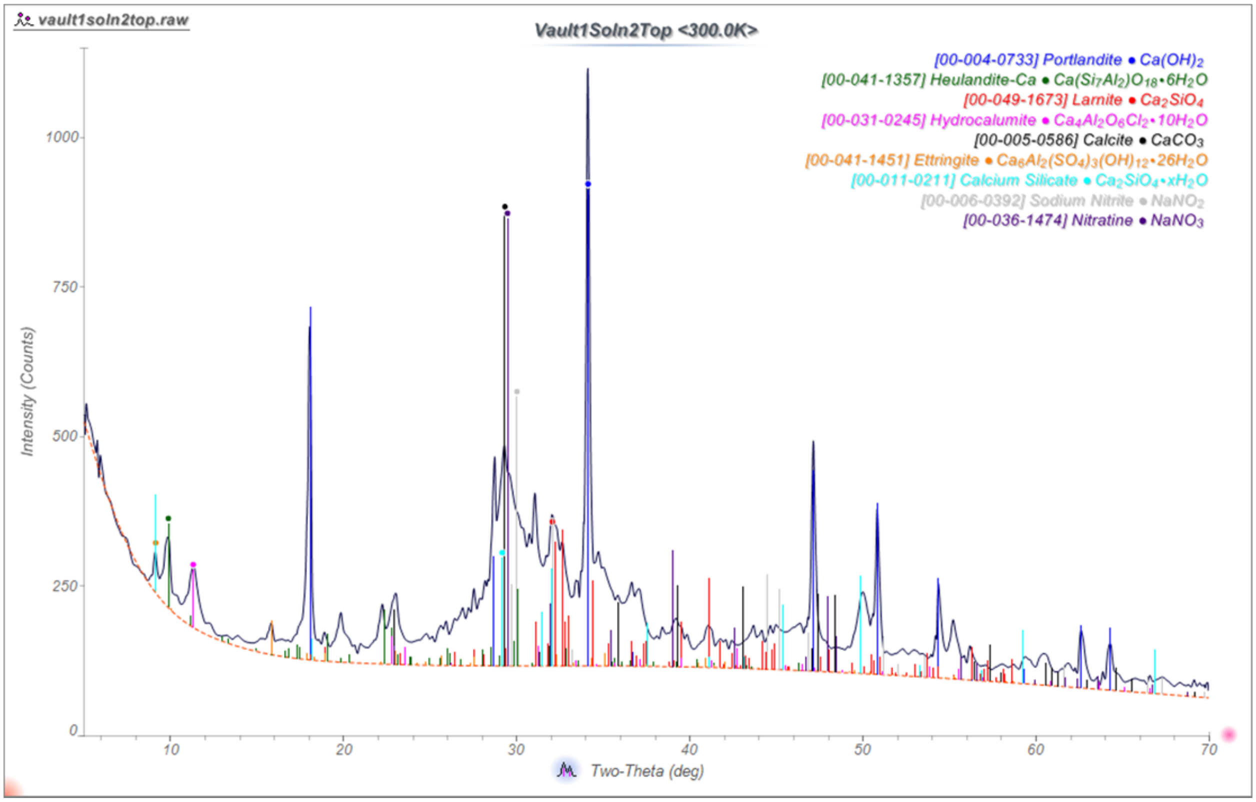
vault1soln2top.raw
Vault1Soln2Top <300.0K>
[00-004-0733] Portlandite ● $Ca(OH)_2$
[00-041-1357] Heulandite-Ca ● $Ca(Si_7Al_2)O_{18}\cdot 6H_2O$
[00-049-1673] Larnite ● Ca_2SiO_4
[00-031-0245] Hydrocalumite ● $Ca_4Al_2O_6Cl_2\cdot 10H_2O$
[00-005-0586] Calcite ● $CaCO_3$
[00-041-1451] Ettringite ● $Ca_6Al_2(SO_4)_3(OH)_{12}\cdot 26H_2O$
[00-011-0211] Calcium Silicate ● $Ca_2SiO_4\cdot xH_2O$
[00-006-0392] Sodium Nitrite ● $NaNO_2$
[00-036-1474] Nitratine ● $NaNO_3$
Intensity (Counts)
1000
750
500
250
0
10
20
30
40
50
60
70
Two-Theta (deg)

PV1S4

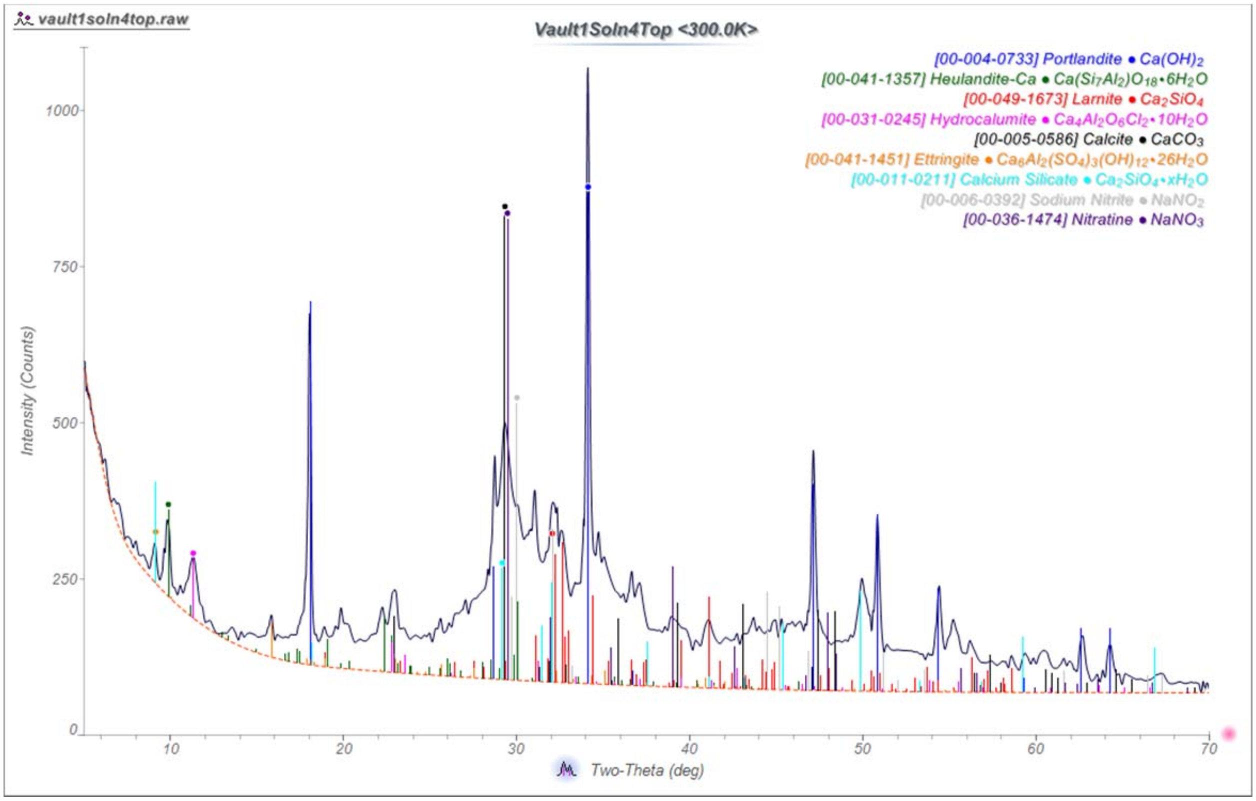
vault1soln4top.raw
Vault1Soln4Top <300.0K>
[00-004-0733] Portlandite • Ca(OH)2
[00-041-1357] Heulandite-Ca • Ca(Si7Al2)O18•6H2O
[00-049-1673] Larnite • Ca2SiO4
[00-031-0245] Hydrocalumite • Ca4Al2O6Cl2•10H2O
[00-005-0586] Calcite • CaCO3
[00-041-1451] Ettringite • Ca6Al2(SO4)3(OH)12•26H2O
[00-011-0211] Calcium Silicate • Ca2SiO4•xH2O
[00-006-0392] Sodium Nitrite • NaNO2
[00-036-1474] Nitratine • NaNO3
Intensity (Counts)
1000
750
500
250
0
10
20
30
40
50
60
70
Two-Theta (deg)

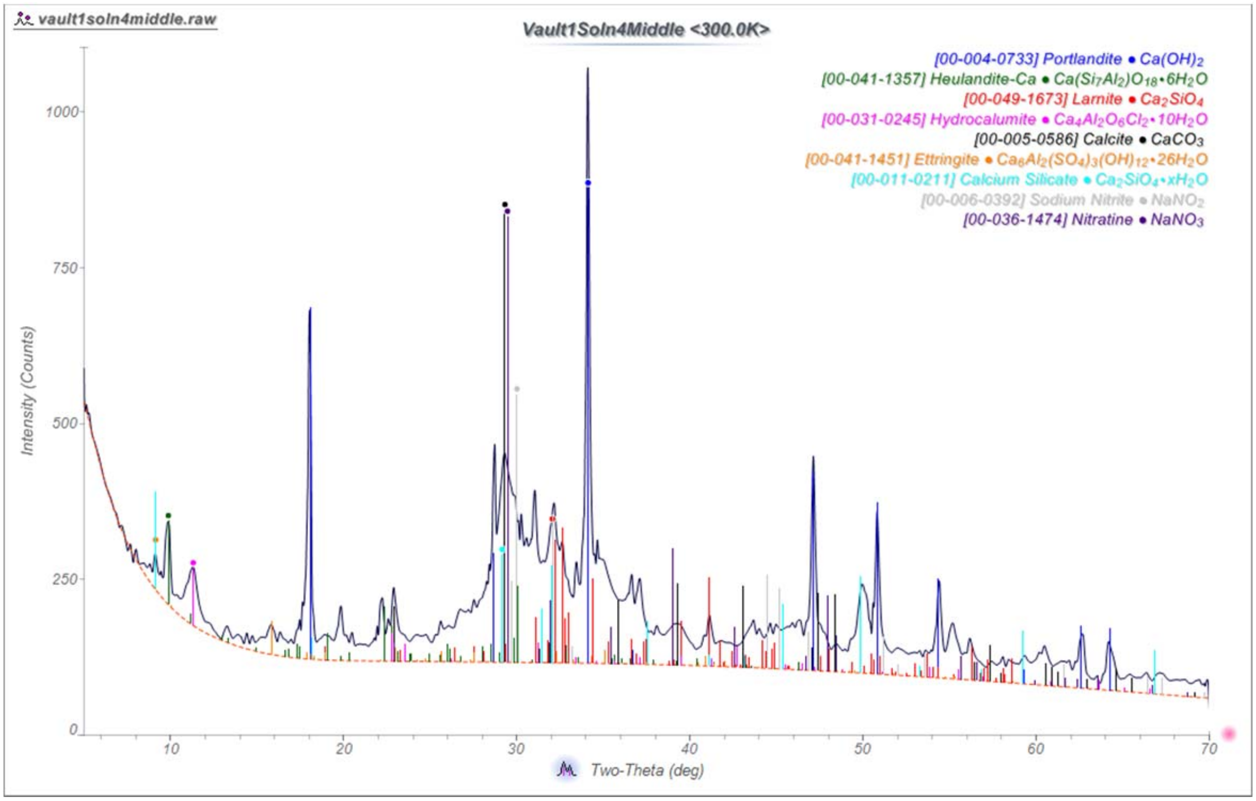
vault1soln4middle.raw
Vault1Soln4Middle <300.0K>
[00-004-0733] Portlandite • Ca(OH)2
[00-041-1357] Heulandite-Ca • Ca(Si7Al2)O18•6H2O
[00-049-1673] Larnite • Ca2SiO4
[00-031-0245] Hydrocalumite • Ca4Al2O6Cl2•10H2O
[00-005-0586] Calcite • CaCO3
[00-041-1451] Ettringite • Ca6Al2(SO4)3(OH)12•26H2O
[00-011-0211] Calcium Silicate • Ca2SiO4•xH2O
[00-006-0392] Sodium Nitrite • NaNO2
[00-036-1474] Nitratine • NaNO3
Intensity (Counts)
1000
750
500
250
0
10
20
30
40
50
60
70
Two-Theta (deg)

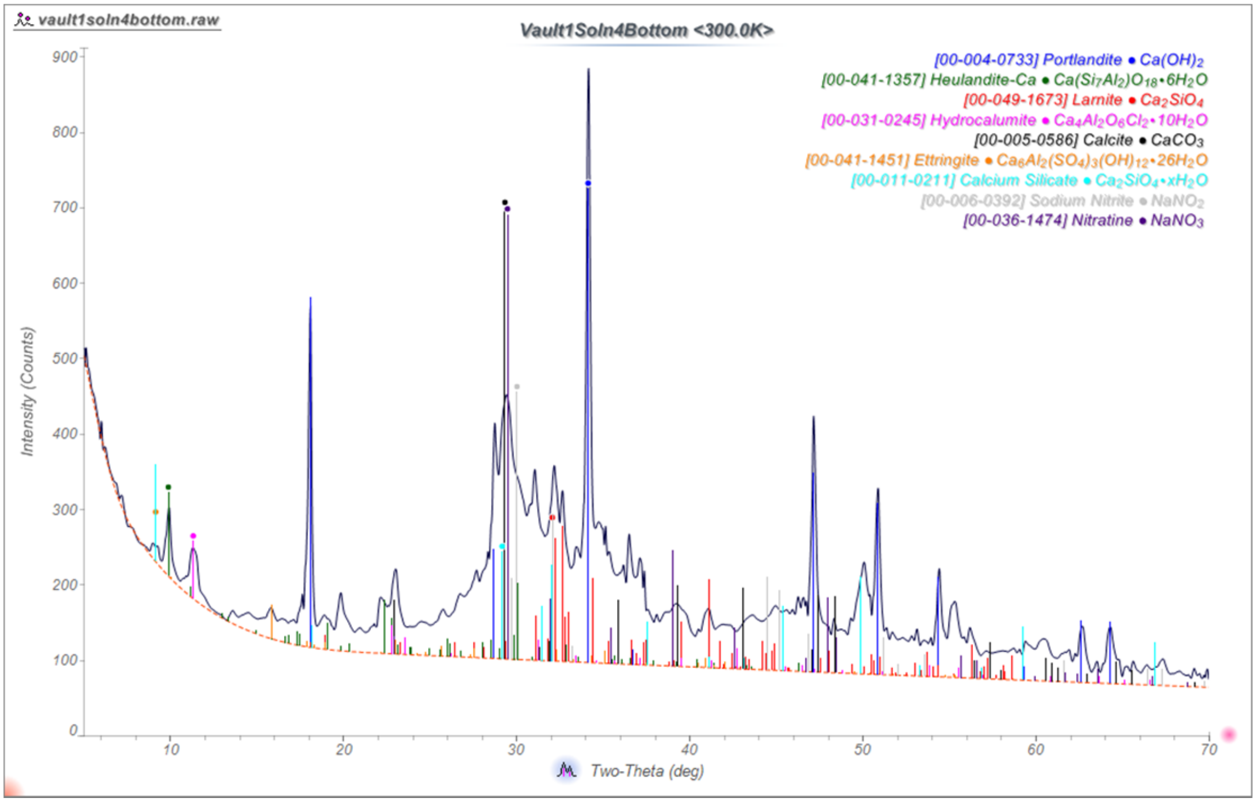

Peak overlap and broad amorphous peak between 25 and 40 °Θ along with incorrect chemical input resulted in database misidentification of $NaNO_2$ and $NaNO_3$ in these patterns

PV2S2

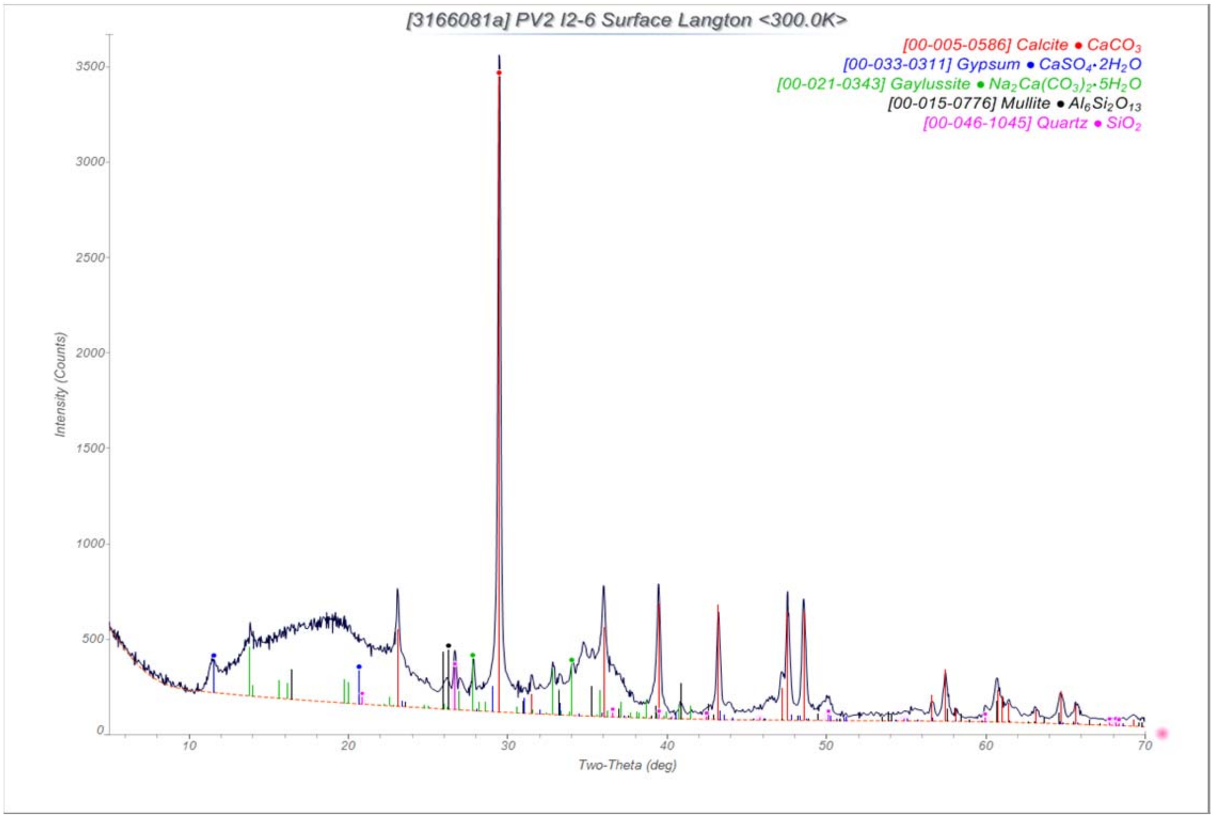
[3166081a] PV2 I2-6 Surface Langton <300.0K>
[00-005-0586] Calcite ● CaCO3
[00-033-0311] Gypsum ● CaSO4·2H2O
[00-021-0343] Gaylussite ● Na2Ca(CO3)2·5H2O
[00-015-0776] Mullite ● Al6Si2O13
[00-046-1045] Quartz ● SiO2
Intensity (Counts)
3500
3000
2500
2000
1500
1000
500
0
Two-Theta (deg)
10
20
30
40
50
60
70

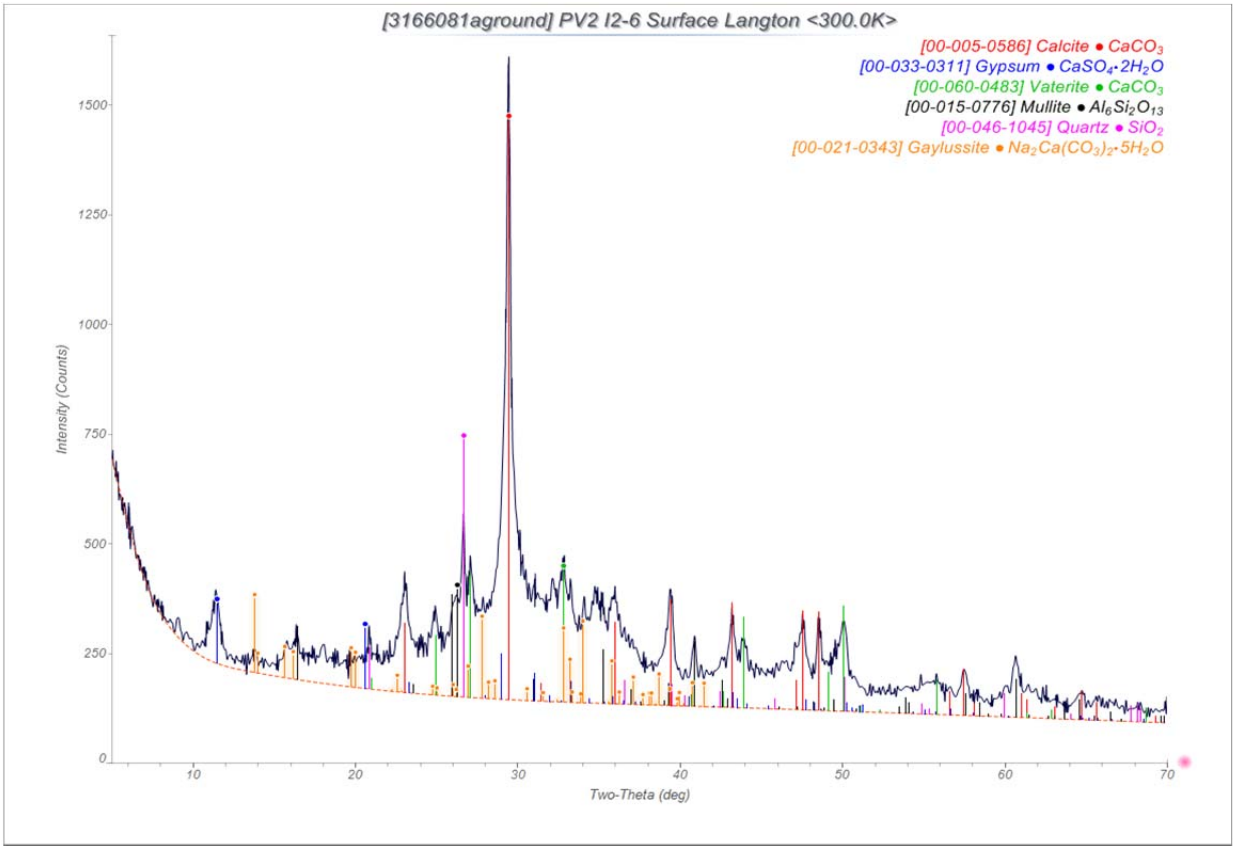
[3166081aground] PV2 I2-6 Surface Langton <300.0K>
[00-005-0586] Calcite ● CaCO3
[00-033-0311] Gypsum ● CaSO4·2H2O
[00-060-0483] Vaterite ● CaCO3
[00-015-0776] Mullite ● Al6Si2O13
[00-046-1045] Quartz ● SiO2
[00-021-0343] Gaylussite ● Na2Ca(CO3)2·5H2O
Intensity (Counts)
1500
1250
1000
750
500
250
0
Two-Theta (deg)
10
20
30
40
50
60
70

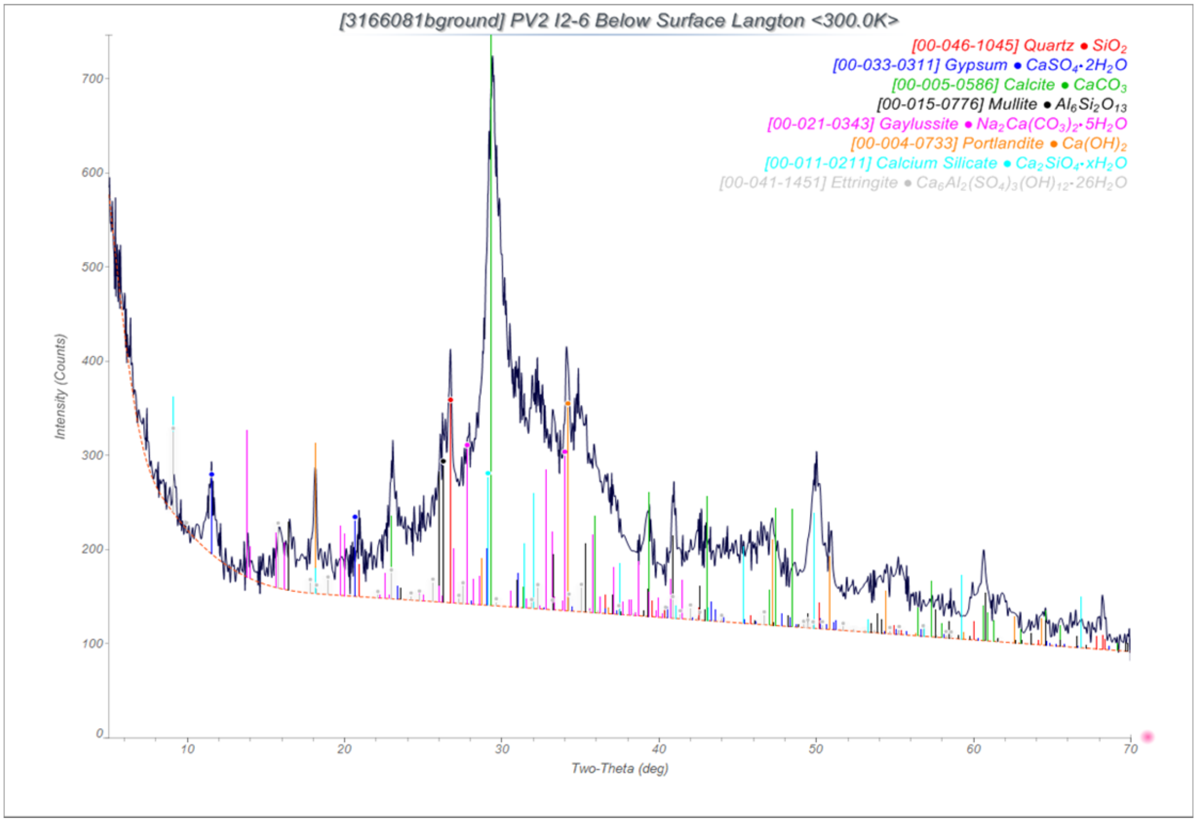
[3166081bground] PV2 I2-6 Below Surface Langton <300.0K>
[00-046-1045] Quartz ● SiO_2
[00-033-0311] Gypsum ● $CaSO_4{\cdot}2H_2O$
[00-005-0586] Calcite ● $CaCO_3$
[00-015-0776] Mullite ● $Al_6Si_2O_{13}$
[00-021-0343] Gaylussite ● $Na_2Ca(CO_3)_2{\cdot}5H_2O$
[00-004-0733] Portlandite ● $Ca(OH)_2$
[00-011-0211] Calcium Silicate ● $Ca_2SiO_4{\cdot}xH_2O$
[00-041-1451] Ettringite ● $Ca_6Al_2(SO_4)_3(OH)_{12}{\cdot}26H_2O$
Intensity (Counts)
700
600
500
400
300
200
100
0
10
20
30
40
50
60
70
Two-Theta (deg)

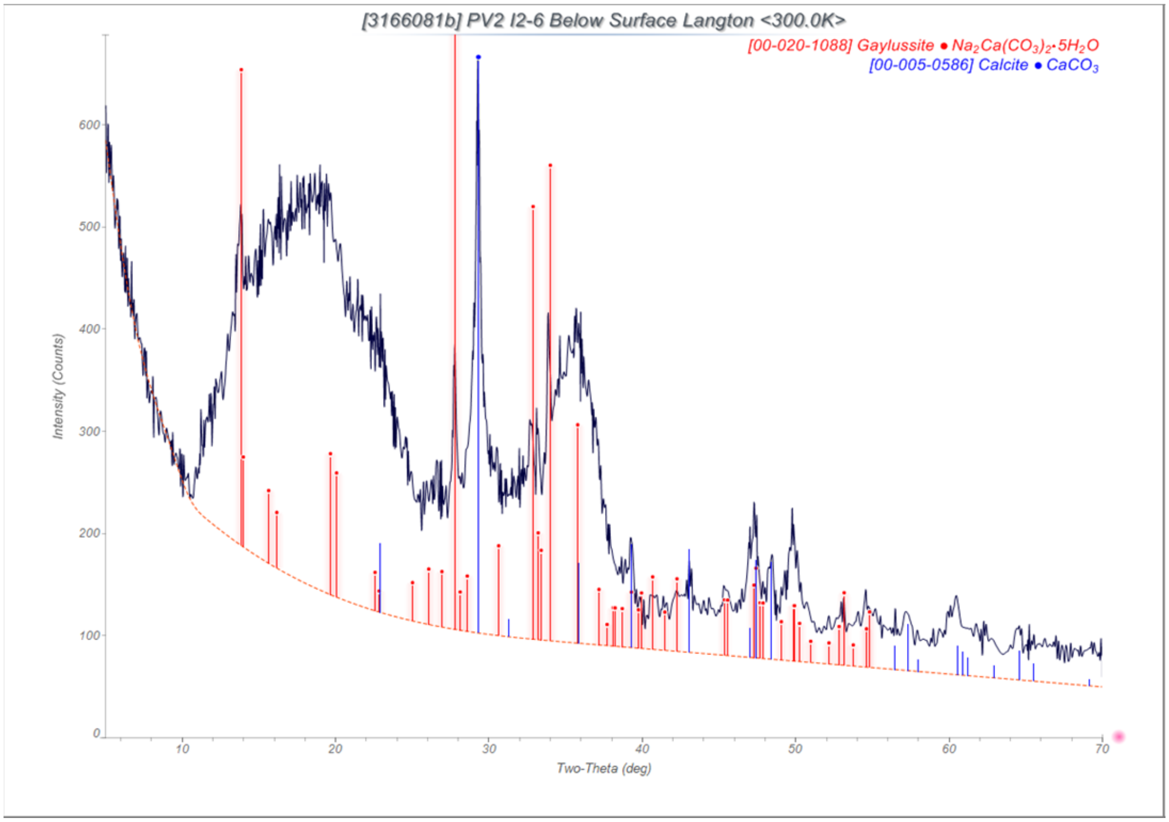
[3166081b] PV2 I2-6 Below Surface Langton <300.0K>
[00-020-1088] Gaylussite ● $Na_2Ca(CO_3)_2{\cdot}5H_2O$
[00-005-0586] Calcite ● $CaCO_3$
Intensity (Counts)
600
500
400
300
200
100
0
10
20
30
40
50
60
70
Two-Theta (deg)

PV2S4

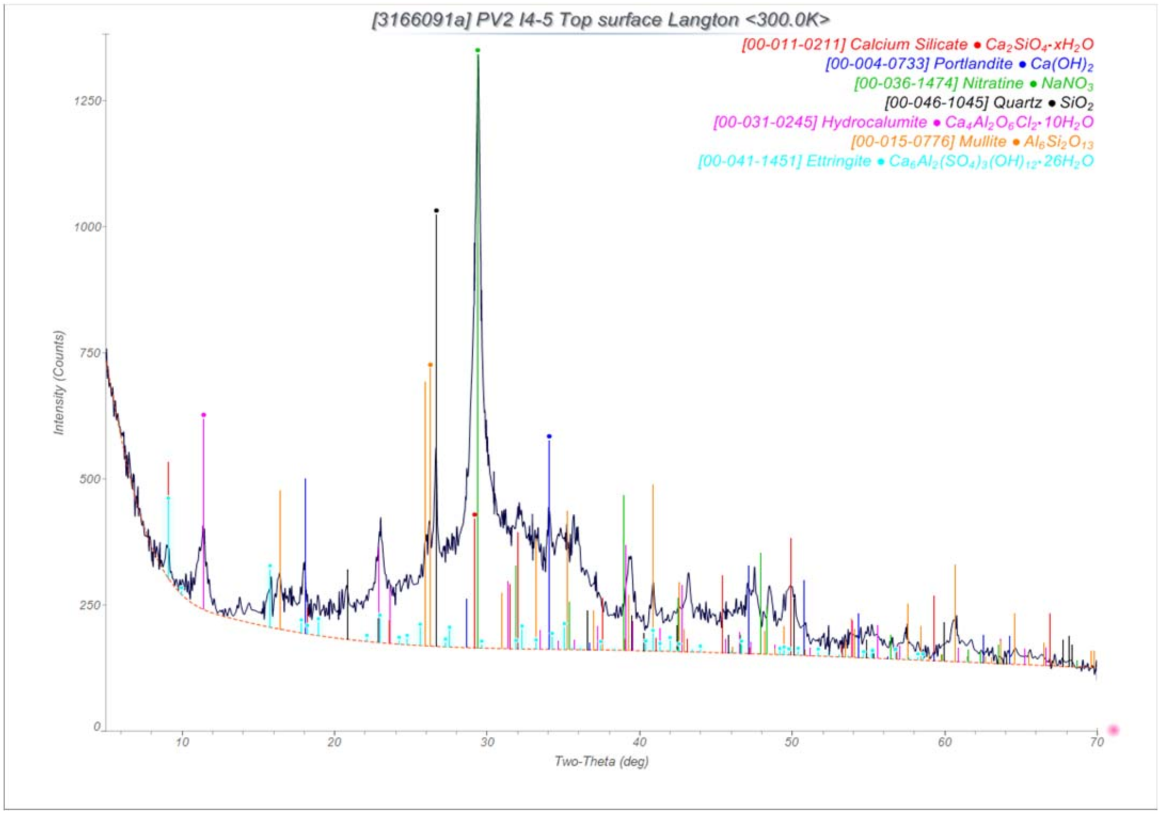
[3166091a] PV2 I4-5 Top surface Langton <300.0K>
[00-011-0211] Calcium Silicate ● $Ca_2SiO_4{\cdot}xH_2O$
[00-004-0733] Portlandite ● $Ca(OH)_2$
[00-036-1474] Nitratine ● $NaNO_3$
[00-046-1045] Quartz ● SiO_2
[00-031-0245] Hydrocalumite ● $Ca_4Al_2O_6Cl_2{\cdot}10H_2O$
[00-015-0776] Mullite ● $Al_6Si_2O_{13}$
[00-041-1451] Ettringite ● $Ca_6Al_2(SO_4)_3(OH)_{12}{\cdot}26H_2O$
Intensity (Counts)
1250
1000
750
500
250
0
10
20
30
40
50
60
70
Two-Theta (deg)

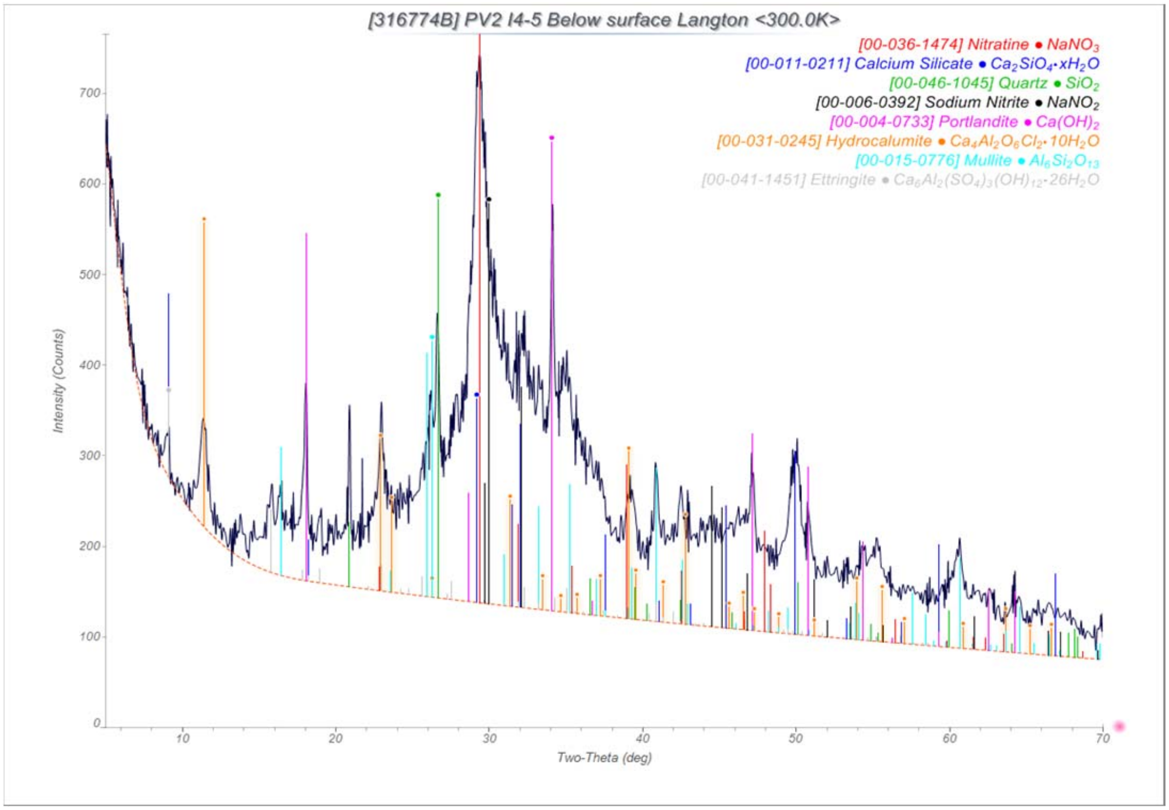
[316774B] PV2 I4-5 Below surface Langton <300.0K>
[00-036-1474] Nitratine ● $NaNO_3$
[00-011-0211] Calcium Silicate ● $Ca_2SiO_4{\cdot}xH_2O$
[00-046-1045] Quartz ● SiO_2
[00-006-0392] Sodium Nitrite ● $NaNO_2$
[00-004-0733] Portlandite ● $Ca(OH)_2$
[00-031-0245] Hydrocalumite ● $Ca_4Al_2O_6Cl_2{\cdot}10H_2O$
[00-015-0776] Mullite ● $Al_6Si_2O_{13}$
[00-041-1451] Ettringite ● $Ca_6Al_2(SO_4)_3(OH)_{12}{\cdot}26H_2O$
Intensity (Counts)
700
600
500
400
300
200
100
0
10
20
30
40
50
60
70
Two-Theta (deg)

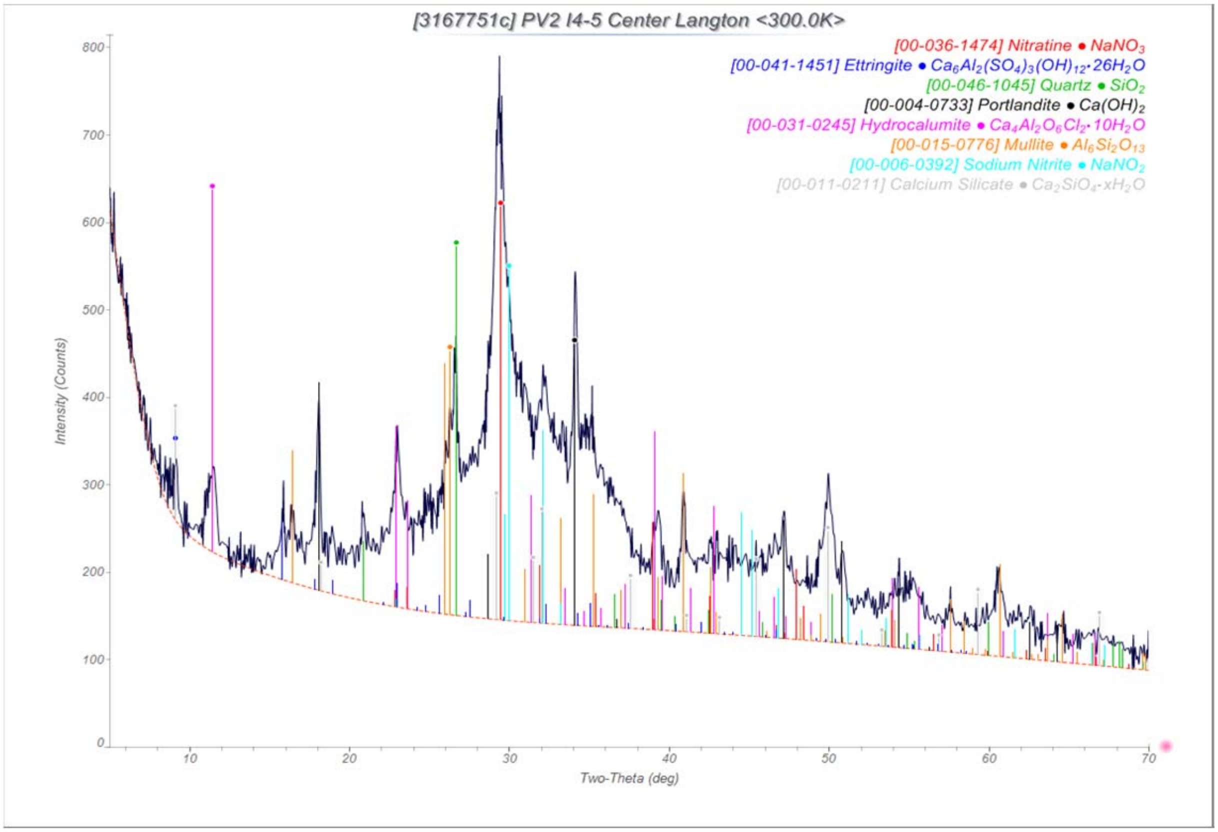
[3167751c] PV2 I4-5 Center Langton <300.0K>
[00-036-1474] Nitratine ● NaNO3
[00-041-1451] Ettringite ● Ca6Al2(SO4)3(OH)12·26H2O
[00-046-1045] Quartz ● SiO2
[00-004-0733] Portlandite ● Ca(OH)2
[00-031-0245] Hydrocalumite ● Ca4Al2O6Cl2·10H2O
[00-015-0776] Mullite ● Al6Si2O13
[00-006-0392] Sodium Nitrite ● NaNO2
[00-011-0211] Calcium Silicate ● Ca2SiO4·xH2O
Intensity (Counts)
800
700
600
500
400
300
200
100
0
10
20
30
40
50
60
70
Two-Theta (deg)

DISTRIBUTION:

H.H. Burns, 773-41A
N.F. Chapman, 766-H
D.E. Dooley, 999-W
G.P. Flach, 773-42A
B.J. Gutierrez, 704-S
E.N. Hoffman, 999-W
D. Kosson, David.Kosson@Vanderbilt.Edu
C.L. Leung, 707-13E
M.E. Maryak, 707-16E
D.L. McClane, 999-W
P. Mallick, DOE-EM, pramod.mallick@em.doe.gov
Y. Protiere, SIMCO Technologies, Inc., yprotiere@simcotechnologies.com
K.H. Rosenberger, 705-1C
S.R. Ross, 704-S
E. Samson, SIMCO Technologies, Inc., esamson@simcotechnologies.com
R.R. Seitz, 773-42A
S. P. Simner, 705-1C
P.C. Suggs, 704-S